8-19-2014 12:00 AM

Elucidating the Signalling Pathway of Mer Tyrosine Kinase Receptor in Efferocytosis

Ekenedelichukwu Azu, *The University of Western Ontario*

Supervisor: Dr. Bryan Heit, *The University of Western Ontario*

A thesis submitted in partial fulfillment of the requirements for the Master of Science degree in Microbiology and Immunology

ELUCIDATING THE SIGNALLING PATHWAY OF MER TYROSINE KINASE RECEPTOR IN EFFEROCYTOSIS

Thesis format: Monograph

by

Ekenedelichukwu Azu

Graduate Program in Microbiology and Immunology

A thesis submitted in partial fulfillment
of the requirements for the degree of
Master of Science

The School of Graduate and Postdoctoral Studies
The University of Western Ontario
London, Ontario, Canada

Abstract

Efferocytosis is the clearance of apoptotic cells and is necessary for homeostasis. Mer Tyrosine Kinase (MerTK) is a crucial efferocytic receptor whose loss is associated with chronic inflammatory diseases and autoimmunity. While previous studies have shown that MerTK mediates efferocytosis through a unique mechanism that requires integrins, MerTK signalling pathway remains unknown. Given this unusual internalization mechanism, I hypothesized that MerTK signals and engages integrins through a novel signalling pathway different from that used by other phagocytic receptors. Therefore, this study aimed to identify the signalling pathways activated by MerTK, utilizing conventional cell biology and pharmacological approaches.

I found that M0 and M2, but not M1 primary human macrophages, expressed MerTK. Moreover, crosslinking MerTK induced endocytosis in a MerTK-dependent manner, which was independent of the common regulators of phagocytosis. Furthermore, crosslinking MerTK resulted in intracellular tyrosine phosphorylation partially dependent on Syk/Src-family kinases and PI3-kinase, which denote their importance in MerTK tyrosine phosphorylation.

Keywords:

MerTK, atherosclerosis, autoimmunity, phagocytosis, efferocytosis, apoptotic cells, tyrosine phosphorylation, endocytosis, Syk/Src-family kinases, PI3-kinase

Acknowledgments

I express my sincere gratitude to my supervisor, Dr. Bryan Heit, for editing my thesis and his overall assistance in this research. Dr. Ron Flannagan has been an integral part of this research; his technical advice and assistance in cloning are greatly appreciated.

I am very grateful for the guidance I received from my advisory committee members, Dr. Sung Kim and Dr. Lakshman Gunaratnam, as well as the Microbiology and Immunology department. It has been a wonderful experience working with my lab members. Many thanks to all those who volunteered for blood donation for peripheral blood mononuclear cell preparation. Lastly, I would like to acknowledge my family for supporting me in all my academic endeavours.

Table of Contents

List of Tables

List of Figures

Chapter 1: Introduction

Efferocytosis is the engulfment of apoptotic cells by phagocytes and is necessary for the maintenance of homeostasis. Apoptotic cells present "eat-me" signals on their cell membrane which act as ligands to enable their recognition by phagocytic receptors. These receptors mediate the uptake and degradation of apoptotic cells in an anti-inflammatory and non-immunogenic fashion. If efferocytosis is defective, apoptotic cells remain uncleared and eventually undergo secondary necrosis. This releases pro-inflammatory intracellular contents and self-antigens into the surrounding tissues, and suppresses the secretion of anti-inflammatory cytokines, thereby promoting inflammation and autoimmunity [1]. MerTK plays an important role in efficient efferocytosis and is required for prevention of the damaging effects of incomplete efferocytosis. Indeed, studies of MerTK mutants and genome-wide association studies have shown MerTK to be critical in the prevention of chronic inflammatory diseases such as atherosclerosis and autoimmune disorders such as lupus [2,3].

1.1 Apoptosis signalling pathway

Apoptosis is defined as programmed cell death that occurs as a normal part of development and homeostasis of cell population [4]. There are two main pathways of apoptosis: the extrinsic pathway which is triggered by pro-apoptotic ligands (example, first apoptosis signal ligand,) binding onto death receptors (example, first apoptosis signal), and the intrinsic pathway, which induces apoptosis in response to noxious cellular stimuli generated by free radicals or lack of growth factors. Both pathways activate cysteine-aspartic proteases (caspases) that play crucial role in apoptosis [2]. Caspases are synthesized in inactive forms called pro-caspases in which their catalytic domains are inhibited by the adjacent pro-domains [5,6]. Activation occurs when the pro-domain of the caspase is cleaved, thus uninhibiting the proteolytic domain. Caspases can be divided into two classes: initiator and effector caspases. Initiator caspases (caspase-8, 9, and 10) cleave and activate other caspases, while effector caspases (caspase-3, 6, and 7) cleave other cellular effectors that mediate the cellular changes associated with apoptosis [5]. These effectors are important in mediating the removal of apoptotic cells. For

example, caspase-3 targets caspase-activated DNase, which degrades DNA during apoptosis, allowing the nuclear components to be dispersed throughout the forming apoptotic bodies. Many other effector proteins are involved in the degradation and packaging of apoptotic cellular materials [7,8]. The combined activity of these proteins produces the typical morphological hallmarks of apoptosis such as nuclear fragmentation, deliberate disassembly of subcellular organelles, re-distribution of plasma membrane lipids, and packaging of cellular contents into blebs. Apoptotic blebs are protrusions of plasma membrane that form by actin-myosin contraction of the cortical actin cytoskeleton. These blebs contain the degraded cytoplasmic materials and organelles produced during apoptosis, and pinch off from the apoptotic cell to form apoptotic bodies which can then be efferocytosed [9,10]. The small size of apoptotic bodies make them easy targets for phagocytes, being much easier for phagocytes to engulf than intact cells.

1.2 Recognition, engulfment, and processing of apoptotic cells

The identification and removal of apoptotic cells is a three-step process in which phagocytes are recruited to the site of apoptosis by "find-me" signals, engage and engulf the apoptotic cell through "eat-me" signals displayed on the apoptotic cell surface, and finally degrade the apoptotic cell. In the first step of this process, apoptotic cells release find-me signals which act as chemoattractants to recruit phagocytes. These find-me signals include ATP, UTP, fractalkine, lysophosphatidylcholine (LPC), and sphingosine-1-phosphate [11]. The mechanisms leading to the release of most of these find-me signals are not well understood, with the exception of LPC which is released from apoptotic cells by a caspase-8-dependent activation of phospholipase A_2 (PLA_2). PLA_2 cleaves phosphatidylcholine to LPC then LPC binds to the G-protein-coupled receptor, G2A, found on phagocytes such as macrophages, thereby enabling macrophage recruitment to the vicinity of the apoptotic cell [7,12]. ATP and UTP signals through purinergic G-protein-coupled receptors such as P2Y2, but their mechanism of release from apoptotic cells remains unclear [13]. Fractalkine is only released by a few subsets of apoptotic cells, typically being released from apoptotic immune cells, and signals through the CX3CR1 chemokine receptor [14].

Binding and engulfment of apoptotic cells are mediated by binding of "eat-me" signals on the apoptotic cell to efferocytic receptors on the phagocyte. Among these eat-me signals are phosphatidylserine, calreticulin, oxidized lipids and DNA. In most healthy cells, phosphatidylserine is confined to the inner leaflet of plasma membrane [9,15]. This plasma membrane asymmetry is lost during apoptosis through the activation of lipid scramblases, leading to the exposure of normally intracellular lipids on the surface of apoptotic cells. Phosphatidylserine exposure is insufficient for efferocytosis, as evidenced by the presence of phosphatidylserine on healthy T and B-cells and on platelets [16,17]. Efferocytosis of these cells is impaired, in part, by the presence of "don't-eat-me" signals such as CD31 and CD47, which are shed or otherwise downregulated during apoptosis [11,16]. Moreover, the concordant recognition of multiple eat-me signals may provide sufficient pro-efferocytic signalling to overcome the inhibitory effect of these don't-eat-me receptors. While phosphatidylserine is the best understood eat-me signal, it is clear that other eat-me signals play an important role in efferocytosis. Characterization of the other eat-me signals is on-going, but it is established that calreticulin is transported from the endoplasmic reticulum to the plasma membrane following endoplasmic reticulum stress, likely via the canonical endoplasmic reticulum-golgi secretion pathway [14,18]. Oxidized LDL are generated by apoptosis-induced oxidants, and are recognized by efferocytic receptors including CD36 and other scavenger receptors [19]. Although controversial, there is some evidence that mitochondrial or nuclear DNA may be exposed on the cell surface where it then acts as an eat-me signal which engages CD91 receptor [20]. Some efferocytic receptors directly bind to these eat-me signals while others require bridging molecules. For example, T-cell Immunoglobulin Mucin family, Brain-specific Angiogenesis Inhibitor-1 , and Stablin-2 receptors directly bind to phosphatidylserine on apoptotic cells [21–23], while MerTK and $\alpha_v\beta_3$ integrin bind to phosphatidylserine through bridging molecules [16].

After recognizing eat-me signals on apoptotic cells, the phagocyte internalizes the apoptotic cell through actin reorganization, leading to the apoptotic cells being internalized into a membrane-bound vacuole termed efferosome in which it is degraded. It is not fully established how this degradation is achieved, but evidence from our lab demonstrates that efferosome maturation progresses through the canonical Rab5-Rab7

maturation pathway, but then recruits novel trafficking regulators at the lysophagosomal stage which may act to direct apoptotic-cell derived antigens away from MHC loading compartments. These experiments demonstrated that many of the regulators and vesicle fusion events that regulate the processing of phagocytic and endocytic cargos are required for the degradation of apoptotic cells (example, Rab5, Rab7, lysosomal fusion; reviewed in [24]). We also found that unique proteins were recruited to the maturing efferosomes, perhaps accounting for the lack of antigen presentation and inflammation following efferocytosis (unpublished data, work by Y. Kim).

1.3 General characteristics of MerTK

1.3.1 MerTK structure and signalling

MerTK is a receptor tyrosine kinase consisting of an extracellular domain with two immunoglobulin-like domains and two fibronectin III motifs, a transmembrane domain, and an intracellular kinase domain [25]. It shares these features with Tyro-3 and Axl receptors making it part of the TAM (Tyro-3, Axl, Mer) subfamily [26]. MerTK is expressed in cells of myeloid, epithelial, and reproductive origin. In the myeloid lineage, it is expressed in macrophages, dendritic cells, and platelets [27]. Furthermore, overexpression of MerTK has been associated with oncogenic transformation in human malignancies such as colon, esophageal, and lung cancers [28].

MerTK is required for normal clearance of apoptotic cells, as shown by Sather, *et al.* [25] where soluble MerTK inhibited clearance of apoptotic cells. It is common for membrane-bound receptors to generate a soluble form through proteolytic cleavage of the extracellular domain by metalloproteinase [25]. This proteolytic cleavage of receptor tyrosine kinases generally functions to limit signalling through the receptor by eliminating the receptor's ligand-binding capabilities, thus contributing to homeostasis through maintaining normal levels of the receptor tyrosine kinases [25]. However, this cleavage can also impair receptor-mediated processes if excessive cleavage occurs. The study by Sather *et al.* [25] revealed that the extracellular domain of MerTK was cleaved by the metalloproteinase, TNF-α Converting Enzyme (TACE), resulting in a soluble form of MerTK. This cleavage was induced *in vitro* after treatment of the cells with phorbol

myristate acetate and lipopolysaccharide (LPS). The shed extracellular domain of MerTK then acted as a decoy receptor by binding to and sequestering Growth Arrest Specific-6 (Gas-6). Sequestering Gas-6 was sufficient to impair MerTK activation, and thus impede macrophage engulfment of apoptotic cells [25]. This was confirmed by addition of TNF-α Processing Inhibitor-0, a TACE inhibitor, which blocked MerTK shedding and restored normal efferocytosis.

1.3.2 MerTK opsonins

The importance of opsonins to MerTK function was first identified in platelets. MerTK ligation induces platelet degranulation and aggregation, thus mice lacking MerTK have platelet dysfunctions [29]. Investigations into the natural ligand that induced MerTK-dependent platelet aggregation led to the discovery that MerTK was not directly binding phosphatidylserine on activated platelets but was interacting via the opsonin, Gas-6. Later studies showed that MerTK not only engaged degranulating platelets, but also apoptotic cells, and revealed several other opsonins, such as Protein S, Tubby, and Tubby-Like Protein 1 (Tulp1), which could mediate the interaction between MerTK and apoptotic cells. Gas-6 and Protein S are gamma-carboxylated in a vitamin K-dependent manner, and act to bridge phosphatidylserine on apoptotic cells through their N-terminal Gla domain to MerTK through their C-terminal laminin G-like [30]. Tubby and Tulp1 are phosphatidylinositide-binding intracellular transcription factors that are secreted through a non-canonical secretion pathway in the extracellular milieu [31], and facilitate Retinal Pigment Epithelial (RPE) cells efferocytosis. Caberoy *et al.* [31] demonstrated that Tubby and Tulp1 induce efferocytosis through activating MerTK. Tubby and Tulp1 bind to $PI(4,5)P_2$ on apoptotic cells through their C-terminal Polyphosphate Binding Domain and to MerTK through their N-terminal Muramyl Dipeptide region [31]. The binding of MerTK to opsonins on apoptotic cells results in clustering of MerTK, leading to autophosphorylation of MerTK kinase domain and thus activation of MerTK signalling and internalization of the apoptotic cells [32,33].

1.3.3 Discovery of MerTK as an efferocytic receptor

The function of MerTK was first discovered in the RPE phagocytic model of congenital blindness. The RPE is a monolayer of cells crucial for proper functioning of the retina. Aside from providing a protective layer over top of the photosensitive layer of the eye, RPE cells also clear the eye of apoptotic debris – in particular the continually shed outer segments of photoreceptor cells [34]. This shedding prevents buildup of toxic oxidative products within the photosensitive cells of the eye through an apoptosis-like process in which the oldest portion of the cell (the outer segment disc) is shed, displays eat-me signals, and is then phagocytosed by an adjacent RPE cell [34]. The RPE model was used to define the overall process of efferocytosis: recognition, binding/engulfment, and degradation of the apoptotic target [34]. MerTK was revealed to be central to RPE phagocytosis in these studies. Specifically, researchers studied the causative agent of retinal dystrophy in the Royal College of Surgeon (RCS) rat model (a rat model of recessively inherited retinal degeneration) [34,35]. They found that in these rats, shed photoreceptor rod outer segments were bound by RPE cells but not internalized, leading to a histologically observable accumulation of outer segment debris. D'Cruz *et al.* [35] used positional cloning to identify the retinal dystrophy loci and discovered that this loci contained a mutation in the MerTK gene. An identical phenotype was observed when MerTK was knocked out in mice, confirming the role of the receptor in the RPE model [36]. This phenotype is recapitulated in humans carrying similar recessive mutations in the MerTK loci [37]. This demonstrates that MerTK is an essential receptor in clearance of shed photoreceptor outer segment in the retina, with mutation in MerTK being responsible for some cases of human juvenile retinal dystrophy [35].

1.3.4 MerTK in autoimmunity and inflammation

In addition to its role in maintaining vision through the removal of apoptotic outer rod segments, MerTK plays a broader role in maintaining homeostasis. It is established that when there is a defect in clearance of apoptotic cells, apoptotic cells are left uncleared. Over time these cells lose metabolic capacity, eventually degrading and undergoing secondary necrosis [14]. These uncleared apoptotic cells release intracellular components, some of which are pro-inflammatory, into the extracellular space. These cellular

components, termed alarmins or danger signals, activate immune cells and induce inflammation [38]. Combined with the release of self-proteins, the release of these alarmins may contribute to induction of autoimmunity [38].

Systemic Lupus Erythematous (SLE) is a chronic autoimmune disease closely tied to failures in efferocytosis. SLE patients express a wide range of clinical manifestations affecting multiple systems such as the nervous, respiratory, cardiovascular, and renal system. A key clinical feature of SLE is the presence of anti-nuclear antibodies in patient sera, likely produced in response to the release of DNA and histones during secondary necrosis [7,39]. Cohen *et al.* [3] reported that mice lacking the intracellular kinase domain of MerTK show delayed clearance of exogenously administered apoptotic cells *in vivo*. The mice developed serological manifestation of lupus including autoantibodies to ssDNA, dsDNA, and IgG, and production of rheumatoid factor. This study also observed that since the extracellular portion of MerTK was still intact, apoptotic cells were being bound but not internalized indicating that physical clearance from the intracellular space was the key step in preventing this lupus-like autoimmunity. Therefore, accumulation of apoptotic cell is a stimulus for systemic autoimmune disease [3]. Furthermore, Recarte-Pelz *et al.* [40] examined the genetic profiles and plasma concentrations of Gas-6, Protein S, and soluble forms of TAM receptors in SLE patients. They discovered increased soluble form of Gas-6 and TAM receptors in the SLE patients but decreased soluble form of Protein S, suggesting that opsonin availability and differences in opsonin activity may correlate with disease onset or activity in SLE [40].

In addition to preventing autoimmunity, MerTK also plays a role in preventing chronic inflammatory diseases such as atherosclerosis. Atherosclerosis is a cardiovascular disease characterized by hardening and thickening of the artery due to plaque formation [41]. There is evidence that impaired efferocytosis of dying cells is linked to progression of atherosclerosis [2,42]. The pathophysiology of atherosclerosis begins with infiltration of macrophages and immune cells into the tunica intima of an artery in response to the deposition of Low-Density Lipoprotein (LDL) and the subsequent release of apolipoprotein B-100 in the intima [41]. Macrophages are recruited to these sites, where they internalize the cholesterol-rich LDL (a process that produces severe cell stress),

leading the macrophages to differentiate into foam cells and eventually become apoptotic. These foam cells are not cleared via efferocytosis, leading to an accumulation of secondary necrotic debris in the core of the lesion [2,43]. As the lesion matures it loses stability, eventually rupturing and producing an intravascular thrombus. If this thrombus detach, it can lodge in smaller vessels within the heart or brain producing a myocardial infarct or ischemic stroke, respectively [44].

A key feature of the atherosclerotic environment is the accelerated apoptosis of macrophages and smooth muscle cells along with defective removal of the dying cells, leading to an accumulation of necrotic cells [41]. This accumulation of necrotic cells appears to be due to defective or impaired efferocytosis, as indicated in a study by Thorp *et al.* [43]. In this study, kinase-defective MerTK/ApoE$^{-/-}$ mice macrophages were unable to clear cholesterol-induced apoptotic macrophages *in vitro*, which suggest that MerTK plays an important role in efferocytosis in atheroma. Moreover, Ait-Oufella *et al.* [42] examined the role of MerTK in atherosclerosis by irradiating and reconstituting atherosclerotic-susceptible mice with MerTK$^{-/-}$ or MerTK$^{+/+}$ bone marrow. After the mice were subjected to high fat diet, MerTK$^{-/-}$ mice had apoptotic cell accumulation within atherosclerotic lesion, accelerated lesion development, and a stronger pro-inflammatory immune response. This suggests that MerTK is important for bone marrow-derived cell efferocytosis and control of inflammation [42].

Human studies have linked MerTK with atherosclerosis for instance, the study by Hurtado *et al.* [45] provided a link between Gas-6 and carotid atherosclerosis. Analysis of the genetic link between Single-Nucleotide Polymorphisms (SNPs) and haplotypes in Gas-6-TAM genes and carotid atherosclerosis led to discovery that SNPs in Tyro3 and MerTK were associated with carotid atherosclerosis, which highlights a role of the Gas-6-TAM pathway in atherosclerosis. When Hurtado *et al.* [46] studied mRNA and protein expression of Gas-6, Protein S, and TAM receptors in human atherosclerotic carotid arteries, they noticed increased MerTK and Protein S in the atherosclerotic arteries versus normal arteries. While the source of the MerTK and Protein S was unclear, the expression profile of these genes in healthy individuals would suggest that they are most likely expressed on cells of a myeloid origin example, macrophages infiltrating the lesion site.

The previously mentioned studies demonstrating that MerTK function to reduce cellularity in atherosclerotic plaques suggest that this increased expression of MerTK and Protein S in the atheroma may act to reduce the overall severity of the disease. Together, these studies provide unequivocal evidence of the importance of MerTK and efferocytosis in atherosclerosis.

1.4 Fcγ receptor signal transduction as a putative model of MerTK signalling

While little is known of the signalling of efferocytic receptors such as MerTK, it is likely that they share some commonalities with other internalization pathways. Indeed, phagocytic receptors face many of the same challenges as efferocytic receptors, such as engagement and internalization of large particulate targets, and therefore represent good models of putative efferocytic signalling pathways. Fcγ receptors (FcγR) are among the best understood phagocytic receptors. These receptors recognize the Fc region of IgG-class antibodies, allowing for phagocytosis of antibody-opsonised pathogens [47]. Three classes of Fcγ receptors have been identified: FcγRI, FcγRII, FcγRIII, with each class having multiple isoforms. For instance, FcγRI is a high affinity receptor that can bind to monomeric IgG, it is encoded by three genes (FcγRIA, FcγRIB, and FcγRIC), and is expressed in monocytes and macrophages [48]. FcγRII is also encoded by three genes (FcγRIIA, FcγRIIB, and FcγRIIC) but is a low affinity receptor. Like FcγRII, FcγRIII is a low affinity receptor but is encoded by two genes (FcγRIIIA and FcγRIIIB) [48]. Not all Fcγ receptors are pro-phagocytic, with some such as FcγRIIB binding to IgG but inhibiting particle internalization [49]. While vastly different in structure and affinity, these receptors share a common signalling pathway, with the FcγRI, FcγRIIA, and FcγRIIIA mediating phagocytosis through Immunoreceptor Tyrosine-based Activation Motifs (ITAM), and the inhibitory FcγRIIB negatively regulating this ITAM pathway via Immunoreceptor Tyrosine-based Inhibition Motifs (ITIM) [48].

Phagocytosis by FcγRs is initiated by binding of antibody-coated particle by these receptors, leading to clustering of the receptors. Signalling is initiated by phosphorylation of two tyrosine residues in the ITAM motifs by members of the Src-family of kinases. Phosphorylation of ITAMs provides binding sites for the SH2-containing kinase, Syk,

which then mediates downstream signalling [16] (Figure 1). This pathway is central to FcγR-mediated phagocytosis as indicated by severe phagocytic deficits in $Syk^{-/-}$ mice, which are completely unable to internalize IgG-opsonised particles [50].

Phosphorylation and activation of Syk leads to recruitment of additional signalling adaptor proteins to the FcγR complex. The transmembrane protein Linker of Activated T-cell (LAT) directly binds to activated Syk and its phosphorylation induces recruitment of other adaptor proteins such as Grb2 and Gab2 to the complex [16]. Gab2 activates the lipid kinase, Phosphoinositide 3-Kinase (PI3K). CrkII, an adaptor protein, and Syk activates the guanine nucleotide exchange factor, DOCK180, and Vav, respectively, which in turn activates Rac1 (a small guanosine triphosphatase phosphatase) which enables actin remodeling [16] (Figure 1). Lipids play an important role in FcγR-mediated phagocytosis. PI3K quickly accumulates at the site of phagocytic cup and phosphorylates $PI(4,5)P_2$ producing $PI(3,4,5)P_3$ which accumulates in the phagocytic cup [16] (Figure 1). $PI(3,4,5)P_3$ is required for macrophages to engulf large particles (greater than 3μm in diameter), but is dispensable for the uptake of smaller particles [24,51]. Importantly, the inhibitory Fcγ receptor, FcγRIIB, functions by recruiting Src homology 2 domain-containing protein tyrosine phosphatase to its ITIM domain. Intermixing of the inhibitory receptor with engaged activating receptor delivers this ITIM-recruited phosphatase which then antagonizes signalling through the activating receptor's ITAM motifs by dephosphorylating both the ITAMs and the Src-family kinases which act to phosphorylate the ITAMs [16]. This ITAM/FcγR signalling pathway appears to be utilized by other phagocytic receptors [52,53], suggesting it may be a universal pathway used by all receptors involved in large particle ingestion, making it an intriguing model for elucidating the signalling of other phagocytosis-like receptors such as MerTK-mediated efferocytosis.

Another important model of phagocytosis of relevance to the study of MerTK is the integrin-mediated phagocytosis model. Integrins are heterodimeric, transmembrane receptors comprising of an alpha and beta subunit [54,55]. They regulate cell signalling, cell cycle and shape, cell migration, and phagocytosis [56,57]. Integrins act as receptors in both phagocytosis and efferocytosis, although the signalling of these receptors has only been

Figure 1: Core FcγR phagocytic signalling pathways.

The signalling pathway involves binding of the ligand-coated particle onto Fcγ receptor, clustering of the receptors, leading to transmission of downstream signals, and particle internalization by actin-driven process. The dashed arrow indicates indirect activation.

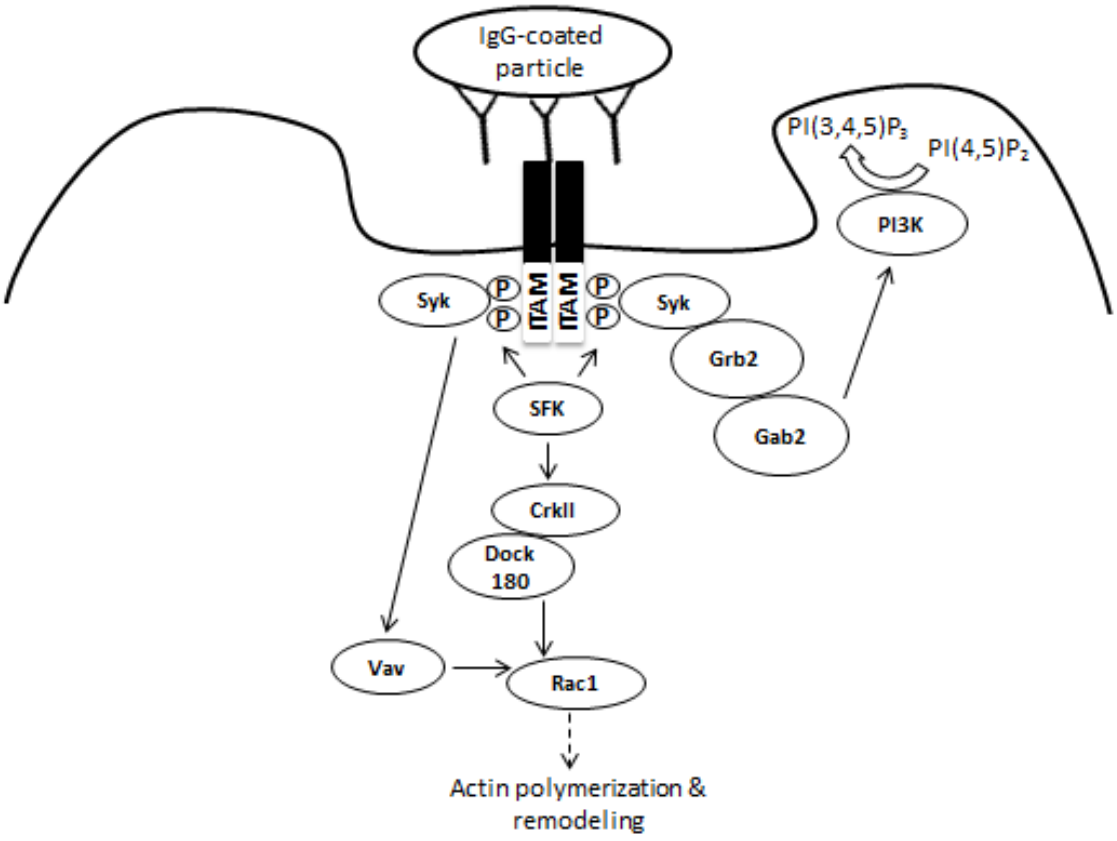
IgG-coated particle
PI(3,4,5)P3
PI(4,5)P2
PI3K
Syk
P
P
ITAM
ITAM
P
P
Syk
Grb2
Gab2
SFK
CrkII
Dock 180
Vav
Rac1
Actin polymerization & remodeling

explored in models of phagocytosis. Importantly to my thesis, the integrins $\alpha_v\beta_3$ and $\alpha_v\beta_5$ are likely involved in MerTK-mediated uptake of apoptotic cells, suggesting that MerTK signalling must intercept the integrin-phagocytic pathway at some point [58,59].

Integrins can signal in two directions: inside-out signalling and outside-in signalling. Inside-out signalling induces the high affinity state of integrins, and is driven by intracellular signalling. Integrins in their inactive state are in a bent conformation that masks their binding domain, creating a low affinity for their ligands. Inside-out signalling occurs when the N-terminal domain of the cytoskeletal protein, talin, binds to the NPX (Y/F) motif in β tail of the integrin, changing its conformation such that the binding site is exposed leading to an increase in its affinity for its ligands [60]. In addition, inside-out signalling can increase the diffusion of integrins, allowing for integrin clustering, leading to a concurrent increase in integrin avidity, and further enhancing integrin-ligand interactions [60]. Outside-in signalling occurs when the high-affinity integrin binds to its ligand. Ligand binding to the extracellular domains of an active integrin recruits a network of proteins, leading to local reorganization of actin cytoskeleton. Regulators of the outside-in signalling pathways include focal adhesion kinase (FAK), Rho GTP-binding proteins, and adaptor proteins such as Cas, Crk, and paxillin [60]. Both the outside-in and inside-out signalling pathways are required for integrin-mediated phagocytosis and may be equally important for MerTK-mediated efferocytosis.

Complement receptor 3, also known as Mac-1 or $\alpha_m\beta_2$, was the first phagocytic integrin to be characterized [16,60]. Phagocytosis by $\alpha_m\beta_2$ requires external stimulatory signals such as chemokines or bacterial products to activate Rap1 (a member of the Ras family of small GTP-binding proteins). This leads to recruitment of talin to the β tail of $\alpha_m\beta_2$ leading to its activation. Bacteria opsonised with complement C3bi binds to $\alpha_m\beta_2$ leading to internalization of the bacteria by RhoA-dependent actin polymerization pathway [16,60]. Following ligation of $\alpha_m\beta_2$, RhoA is activated and recruited to the site of phagocytosis where it activates the serine/threonine kinase, Rho-associated protein kinase (ROCK), which then mediates recruitment of actin-related protein-2/3 and activation of myosin IIA to drive actin polymerization and reorganization. There is evidence that mutation of the β-integrin intracellular tail impedes RhoA activation and thus phagocytosis [56]. In

addition, $\alpha_m\beta_2$ appears to be able to activate the Src/Syk pathway utilized by Fcγ receptors via the ITAM-bearing adaptor proteins, FcRγ and DAP12 [61]. This suggests that a combination of ITAM signalling and RhoA is important for $\alpha_m\beta_2$- mediated phagocytosis and therefore may be important for efferocytosis via the MerTK-integrin pathway.

The integrins identified as being involved in clearance of apoptotic cells are not the same as those involved in phagocytosis. Efferocytic integrins include $\alpha_v\beta_3$ and $\alpha_v\beta_5$ [53,59]. Like MerTK, $\alpha_v\beta_5$ does not directly bind to phosphatidylserine on apoptotic cells but instead is bridged by the opsonin, Milk Fat Globule-EGF factor 8 (MFG-E8), also known as lactadherin (Figure 2). While $\alpha_m\beta_2$-mediated phagocytosis is dependent on RhoA, it is unclear if RhoA plays a role in $\alpha_v\beta_5$ efferocytosis. Moreover, it has not been tested whether the ITAM/Src/Syk pathway is utilized by any efferocytoic receptor. It is established that $\alpha_v\beta_5$ efferocytosis is dependent on Rac1 activation [60], which occurs downstream of ITAMs during FcγR-dependent phagocytosis. $\alpha_v\beta_5$ activates Rac1 by the Dock180-ELMO complex (a cascade that involves p130Cas and CrkII pathway) and the RhoA-related protein, RhoG, all processes thought to be downstream of Src-family kinases and/or ITAMs [26,58]. Critically, Wu *et al.* [58] revealed that neither MerTK nor $\alpha_v\beta_5$ integrin are independently sufficient for efferocytosis, but instead that efferocytosis requires their combined activity. We believe this indicates that MerTK provides the inside-out signal that induces the high affinity state of $\alpha_v\beta_5$, which then engages the apoptotic cell and recruits the full internalization machinery to the forming efferocytic cup through its outside-in signalling (Figure 2) – a possibility to be tested in our future studies.

Figure 2: Schematic of the known $\alpha_v\beta_5$ integrin and MerTK signalling pathway.

MerTK signalling pathway may intersect with $\alpha_v\beta_5$ integrin through activation of FAK by Src-family kinases mediating the internalization of apoptotic cells.

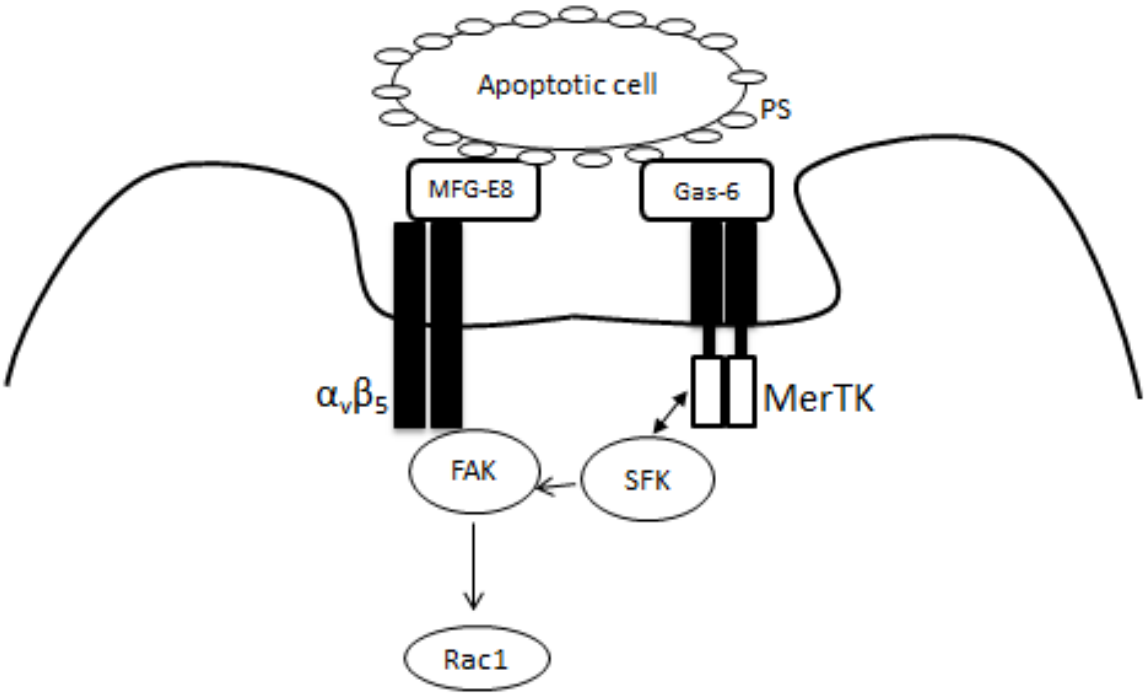
Apoptotic cell
PS
MFG-E8
Gas-6
$\alpha_v\beta_5$
MerTK
FAK
SFK
Rac1

1.5 Hypothesis and objectives

The signalling pathway of MerTK in macrophages remains unknown, but because efferocytosis results in a vastly different immunological outcome compared to phagocytosis, **I hypothesized that MerTK signals and engages integrins through a novel signalling pathway different from that used by other phagocytic receptors.** To address this hypothesis, my initial objectives were to determine if common regulators of phagocytosis/endocytosis regulate MerTK-mediated efferocytosis, and to use phosphotyrosine immunoprecipitation followed by mass spectrometry to identify kinase pathways activated by MerTK ligation. Once the proteins were identified and validated, their signalling dynamics were to be assessed by confocal microscopy of fluorescently-tagged signalling molecules and through siRNA/pharmacological inhibition. Initially, I also proposed to generate tagged and mutagenized variants of MerTK to use in the signalling and immunoprecipitation studies. Lastly, I had planned on comparing the activity of the identified signalling pathways under normal and atherosclerotic conditions thereby identify any defects in MerTK signalling that may account for its role in atherosclerosis.

However, due to difficulties in identifying a cell line with consistent MerTK expression and in generating an ectopic expression model, the project proposal had to be modified. Instead, in my first objective I characterized the expression of endogenous MerTK in primary human macrophages. In my second objective, MerTK endocytosis was induced in M0 primary human macrophages by antibody-crosslinking, and the role of the common phagocytic regulators Src-family kinases, Syk and PI3K in MerTK endocytosis were assessed using pharmacological inhibitors. Thirdly, the role of these signalling pathways was assessed in the induction of MerTK-dependent tyrosine phosphorylation. In the final objective, I sought to immunoprecipitate proteins tyrosine-phosphorylated by MerTK crosslinking, with the goal of identifying these signalling regulators using an unbiased mass spectrometry approach.

Chapter 2: Materials and methods

Chapter 2: Materials and methods

2.1 Murine macrophage cell culture

RAW264.7 and J774.1 murine macrophages were cultured in RPMI-1640 (Wisent) containing 10% Fetal Bovine Serum (Invitrogen). ANA-1 murine macrophages were cultured in Dulbecco's Modified Eagle's Medium (Wisent) supplemented with 10% FBS. All cells were cultured at 37°C in 5% CO_2 and split at 80% confluency. RAW264.7 and J774.1 cells were a gift from S. Grinstein, Hospital for Sick Children, and ANA-1 cells were a gift from M. Valvano, Western University.

2.2 Primary human macrophage cell culture

Blood collection was approved by Western University's Health Sciences Research Ethic Board and complies with the Tri-Council Policy Statement on human research. Human blood was drawn from healthy consenting donors using butterfly blood collection needles and 10mL BD Vacutainer sodium heparin tubes (Thermo Fisher). Blood was layered in 15mL Falcon tubes over an equal volume of Lympholyte-poly cell separation media (Cedarlane), followed by centrifugation at 500 x g for 35 minutes with no brake, and removal of the top band of cells, the peripheral blood mononuclear cells (PBMCs). PBMCs were washed with room-temperature phosphate-buffered saline (PBS) at 300 x g for 6 minutes, diluted with RPMI-1640 containing 10% FBS and antibiotic antimycotic solution (Corning), then plated on 12-well plates with 18mm coverslips placed in the wells or on 6-well plates coated with 0.1% gelatin solution. Cells were incubated at 37°C under 5% CO_2 for 1 hour to allow selective adherence of the PBMCs.

After 1 hour, cells were washed with warm PBS to remove non-adherent cells followed by addition of RPMI-1640 containing 10% FBS, antibiotic antimycotic solution (100X), and differentiated with cytokines (1000X) from R&D Systems: 10ng/mL recombinant human (rh) M-CSF (to obtain M0 & M2) or 20ng/mL rhGM-CSF (to obtain M1), differentiation for 5 days, followed by an additional 2 days of culture with 10ng/mL rhM-CSF (for M0), 20ng/mL rhGM-CSF + 250μg/mL LPS + 100ng/mL IFN-γ (for M1) or 10ng/mL rhM-CSF + 10μg/mL IL-4 (for M2).

2.3 Cloning human MerTK-wild type, mouse MerTK-wild type and GFP, and human HA-MerTK

Human and mouse MerTK cDNA was purchased from the MGC genome collection. PCR was used to amplify MerTK using Phusion High-Fidelity DNA Polymerase (Thermo Scientific) with 35 cycles. Amplification primers were designed with SnapGene software and are listed in Table 1 and 2. PCR products were purified using EZNA Cycle Pure Kit (Omega Biotek). The amplified PCR products and target vectors were digested with their corresponding restriction enzymes (Fermentas), as shown in Table 1 and 2, for 2 hours at 37ºC, purified using Geneclean II EZ-Glassmilk Kit (MP Biomedicals), and then ligated overnight at 16°C using T4 DNA ligase (Fermentas). DNA sequencing was performed by the London Genomics Centre (Robarts Research Institute, London, Canada). Plasmid maps are located in the appendix (Figure A1).

Table 1: Primers for cloning human MerTK-WT, mouse MerTK-WT, and mouse MerTK-GFP

Insert name	**Amplification primer sequence (5' to 3') with restriction sites underlined**	**Restriction Enzyme**	**Target vector**
Human MerTK-WT	**FWD:** AAA AAA GAA TTC ATG GGG CCG GCC C **REV:** AAA AAA ACC GGT TCA CAT CAG GAC TTC TGA GCC TTC T	EcoRI AgeI	pEGFP-N1
Mouse MerTK-WT	**FWD:** AAA AAA GAA TTC ATG GTT CTG GCC CCA CTG **REV:** AAA AAA ACC GGT TCA CAT CAG AAC TTC AGA GTC TTC CAA GG	EcoRI AgeI	pEGFP-N1
Mouse MerTK-GFP	**FWD:** TAT GAA TTC ATG GTT CTG GCC CCA CTG CTA CTG **REV:** GGT GGC GAC CGG TTT CAT CAG AAC TTC AGA GTC TTC CA AGG AGT	EcoRI AgeI	pEGFP-N1

Table 2: Primers for cloning human HA-MerTK

Insert name	**Amplification primer sequence (5' to 3') with restriction sites underlined**	**Restriction Enzyme**	**Target vector**
Upstream half of HA-MerTK	**FWD:** TTT TTT AGA TCT GCT ATC ACT GAG GCA AGG GAA GAA **REV:** GAA GAG GGG GCA TAG TCG ACC CAA CCG TGT GCA GGG ATA AAT	BglII SalI	pDisplay-LAP2
Downstream half of HA-MerTK	**FWD:** ATT TAT CCC TGC ACA CGG TTG GGT CGA CTA TGC CCC CTC TTC **REV:** TTT TTT CTC GAG TCA CAT CAG GAC TTC TGA GCC TTC TGA	SalI XhoI	pBluescript
Full-length HA-MerTK	**FWD:** TTT TTT AGA TCT GCT ATC ACT GAG GCA AGG GAA GAA **REV:** TTT TTT CTC GAG TCA CAT CAG GAC TTC TGA GCC TTC TGA	BglII XhoI	pDisplay-LAP2

Table 3: Antibodies with dilutions and sources

Antibody	**Dilution**	**Source**
Rabbit monoclonal anti-mouse MerTK antibody	1:1000	Abcam
Donkey anti-rabbit IR-700	1:10,000	Jackson ImmunoResearch
Rabbit monoclonal anti-human MerTK	1:1000, 1:500, 1:200	Abcam
Dylight 488-conjugated Fab fragment donkey anti-rabbit IgG	1:1000	Jackson ImmunoResearch
Cy3-conjugated Fab fragment donkey anti-rabbit IgG	1:1000	Jackson ImmunoResearch
Goat anti-human 488 Fab	1:1000	Jackson ImunoResearch
$F(ab')_2$ goat anti-rabbit IgG Fc fragment specific	1:200	Jackson ImmunoResearch
Dylight 488-conjugated Fab anti-mouse	1:1000	Jackson ImmunoResearch
Goat anti-rabbit Cy3-conjugated $F(ab')_2$	1:500	Jackson ImmunoResearch
Mouse monoclonal anti-phosphotyrosine, clone 4G10	1:1000	Millipore

2.4 Immunoblotting for endogenous MerTK on RAW264.7 and J774.1 cells

RAW264.7 and J774.1 cells were plated at approximately 5 x 10^5 cells per 35mm-diameter well and were incubated for 24 hours to obtain approximately 80% confluency. Cells were lysed with 4X Laemmli buffer containing 1/10^{th} volume of β-mercaptoethanol, and protease plus phosphatase inhibitors (100X, Thermo Scientific). Cell lysates were vortexed for 30 seconds, boiled at 100°C for 5 minutes, and ran on a 12% SDS-PAGE for one hour at 110V. Protein bands were transferred onto a nitrocellulose membrane for two hours at 85V, then membrane was blocked with Tris-Buffered Saline with Tween (TBST) plus 5% Bovine Serum Albumin (BSA) for 4 hours. The membrane was probed with rabbit monoclonal anti-mouse MerTK antibody (1:1000, Abcam) for 2 hours and donkey anti-rabbit IR-700 (1:10,000, Jackson ImmunoResearch) for 1 hour. Three-15 minutes washes with TBST followed each antibody incubation step. The membrane was imaged with LI-COR Odyssey Infrared Imaging System.

2.5 Immunostaining for MerTK expression

J774.1 and ANA-1 macrophages were plated at approximately 5 x 10^5 cells per 18mm coverslip on a 12-well plate and were incubated for 24 hours to obtain approximately 80% confluency, while primary human macrophages were cultured onto 12-well plates with coverslip as per "Primary human macrophage cell culture" protocol (Section 2.2). Cells were fixed with 4% PFA at room temperature for 20 minutes then blocked with 1% BSA at room temperature for 30 minutes. Primary human macrophages were immuostained with DAPI (1:1000, Abnova) and rabbit monoclonal anti-human MerTK (1:1000, Abcam) while J774.1 and ANA-1 macrophages were stained with DAPI and rabbit monoclonal anti-mouse MerTK for 1 hour, followed by Dylight 488-conjugated Fab fragment donkey anti-rabbit IgG (1:1000, Jackson ImmunoResearch) and Cy3-conjugated Fab fragment donkey anti-rabbit IgG (1:1000, Jackson ImmunoResearch), respectively. Cells were mounted with PermaFluor and images were acquired using Olympus IX70 inverted fluorescent microscope equipped with a 60X/0.9NA objective and operated by micro-manager software [63], or imaged on a Zeiss LSM510 meta confocal microscope equipped with a 60X/1.0NA objective.

2.6 Co-transfection of HeLa and RAW264.7 cells with pIRES2-EGFP MerTK and mCherry-Rab7

Cells were seeded onto 18mm coverslips placed into the wells of a 12-well plate and incubated for 24 hours at 37°C to obtain approximately 80% confluency. The media on the cells was replaced with fresh media one hour prior to transfection. RAW and HeLa cells were transfected with 1.1µg of each plasmid using FuGENE-HD transfection reagent (Promega). After 24 hours of transfection, the cells were fixed with 4% PFA and mounted with PermaFluor (Thermo Scientific). The pIRES2-EGFP murine MerTK plasmid was purchased from Addgene (#14998). Plasmid map is located in the appendix (Figure A1). Images were captured using Olympus IX70 inverted fluorescent microscope equipped with a 60X/0.9NA objective and operated by micro-manager software [63].

2.7 Phagocytosis assay of M0 primary human macrophages

M0 primary human macrophages were cultured onto a 12-well plate as per "Primary human macrophage cell culture" protocol (Section 2.2). 4.95µm Protein A-coated beads and 5.09µm polystyrene microsphere beads (Bangs Laboratories) were used as phagocytic targets.

Protein A-coated beads were prepared by diluting 10µL of beads with 500µL of 1X PBS. For anti-human MerTK-coated beads, 10µL of the diluted beads was mixed with 2.5µL of rabbit monoclonal anti-human MerTK antibody. For isotype control beads, 10µL of the diluted beads was mixed with 2.5µL of whole human IgG. Beads were rotated for 30 minutes at room temperature, washed with 1mL of 1X PBS, and stained with eFluor 670 Cell Proliferation Dye (1:1000, eBioscience). Beads were washed, re-suspended with 1mL of HEPES RPMI, and added into each well of macrophages. Macrophages were centrifuged at 500 x g for 1 minute then phagocytosis was induced by incubating them at 37ºC for 30 minutes. After incubation, cells were washed with 1X PBS then non-internalized beads were labelled with anti-rabbit 488 Fab, or goat anti-human 488 Fab (Jackson ImmunoResearch) for isotype control. Cells were fixed with 4% PFA for 20 minutes at room temperature, immunostained for MerTK and counterstained with DAPI

as per immunostaining protocol (Section 2.5). After mounting with Permaflour (Thermo Scientific), images were acquired with 60X objective using Olympus IX70 inverted fluorescent microscope.

Polystyrene microsphere beads were prepared by mixing 10µL of the beads with 500µL of PBS, and 2.5µL of $F(ab')_2$ goat anti-rabbit IgG Fc fragment specific antibody (Jackson ImmunoResearch) then rotating for 15 minutes at room temperature. Beads were washed three times with 1X PBS and blocked with 500µL of 5% BSA for 15 minutes, washed thrice again, and then 10µL of beads were re-suspended with 500µL of 1X PBS and rabbit monoclonal anti-human MerTK antibody (1:200, Abcam) or rabbit anti-sheep Far Red for the isotype control. Beads were rotated for 1 hour then washed thrice. Anti-human MerTK beads were labelled with eFluor 670 Cell Proliferation Dye (1:1000, eBioscience). Beads were re-suspended with 1mL of HEPES RPMI. Phagocytosis was induced by adding the 1mL of bead-containing HEPES RPMI into each well of macrophages, centrifuging at 500 x g for 1 minute, and incubating plates at 37°C for 30 minutes. Unbound beads were removed by three washes with 1X PBS then non-internalized external beads were labelled with Dylight 488-conjugated Fab fragment donkey anti-rabbit IgG (1:1000, Jackson ImmunoResearch) for 20 minutes. Cells were washed, fixed with 4% PFA for 20 minutes at room temperature, and mounted with Permaflour. Images were acquired with 60X objective using DIC and Olympus IX70 inverted fluorescent microscope.

2.8 Induction of IgG-mediated phagocytosis by RAW264.7 cells

RAW264.7 macrophages were plated at approximately 5 x 10^5 cells per 18mm coverslip on a 12-well plate and were incubated for 24 hours to obtain approximately 80% confluency. Whole mouse IgG-coated beads were prepared by mixing 10µL of 5.09µm polystyrene microsphere beads (Bangs Laboratories) with 300µL of 1X PBS and 15µL whole mouse IgG then rotating for 1 hour at room temperature. Beads were washed twice and re-suspended with 500µL of 1X PBS then 10µL of coated beads was added to each well of macrophages in 1mL of serum-free HEPES RPMI. The cells were centrifuged at

500 x g for 1 minute then incubated at 37°C for 30 minutes. Unbound beads were removed by two washes with room temperature 1X PBS and non-internalized external beads labelled with anti-mouse Dylight 488 antibody (1:1000; Jackson ImmunoResearch) for 20 minutes. Cells were washed twice, fixed with 4% PFA for 20 minutes at room temperature, and mounted with Permaflour. For inhibition of IgG-mediated phagocytosis, the cells were treated with 50μM LY294002, 50μM piceatannol, and 30μM PP1 for the duration of the experiment. Images were acquired with 60X objective using DIC and Olympus IX70 inverted fluorescent microscope. Phagocytic index was calculated by dividing the total number of internalized beads by total number of macrophages counted. A minimum of 45 macrophages were counted for each condition (untreated, LY294002, piceatannol, and PP1-treated) in one experiment. Images were analyzed on Fiji ImageJ software (http://fiji.sc/Fiji). Graph was created using GraphPad Prism.

2.9 MerTK endocytosis assay

M0 primary human macrophages were cultured onto 18mm coverslips on a 12-well plate as per "Primary human macrophage cell culture" protocol (Section 2.2). Basal levels of endocytosis was inhibited by pre-incubating cells for 4 hours prior to the experiment in serum-free RPMI-1640, and the cells were cooled to 10°C prior to MerTK crosslinking. MerTK was ligated by the addition of rabbit anti-human MerTK (1:500, Abcam) for 20 minutes at 10°C, followed by three washes in 1X PBS, and then crosslinked with goat anti-rabbit Cy3-tagged $F(ab')_2$ (1:500, Jackson ImmunoReaserch). The cells were washed with 37°C RPMI with HEPES and incubated at 37°C for 20 minutes to allow for MerTK internalization. Internalization was stopped by washing the cells with 10°C 1X PBS, and surface-bound antibody was removed by 2 minutes acid-wash (1X PBS, pH 2.0 10°C). Cells were fixed for 20 minutes with 4% PFA at 10°C, co-stained with wheat-germ agglutinin (1:1000) for 5 minutes at 10°C, and then mounted with Permaflour (Thermo Scientific). A sufficient number of fields (4-5 fields, 10 cells/field) were imaged before and after acid washing to ensure a statistically representative sample of MerTK expression and internalization. Images were acquired using Olympus IX70 inverted fluorescent microscope equipped with a 60X/0.9NA objective and operated by micro-manager software [63].

For pharmacological inhibition studies, macrophages were incubated with the PI3K inhibitor LY294002 at 50μM, the Syk inhibitor piceatannol at 50μM, and the Src-family kinase inhibitor PP1 (Tocris Bioscience) at 30μM from 10 minutes prior to internalization until fixation.

2.10 Phosphotyrosine immunostaining

M0 primary human macrophages were cultured as per "Primary human macrophage cell culture" protocol (Section 2.2). Cells were serum starved for 4 hours to reduce basal phosphoprotein levels then cooled at 10°C for 15 minutes. For pharmacological inhibition studies, macrophages were incubated with the PI3K inhibitor LY294002 at 50μM, the Syk inhibitor piceatannol at 50μM, and the Src-family kinase inhibitor PP1 at 30μM, with inhibitors added 20 minutes prior to stimulation and kept on the sample until fixation. Rabbit monoclonal anti-human MerTK (1:500, Abcam) was added to the cells for 20 minutes at 4°C, the cells were washed three times with 4°C 1X PBS then treated with crosslinking goat anti-rabbit Cy3-tagged $F(ab')_2$ (1:500, Jackson ImmunoResearch). Cells were incubated at 4°C for 20 minutes then fixed with 4% PFA for 20 minutes at room temperature. Cells were blocked and permeabilized with 1X PBS + 0.1% Triton X-100 + 5% rat serum for 1 hour at room temperature followed by incubation with mouse monoclonal anti-phosphotyrosine antibody, clone 4G10 (1:1000, Millipore) in blocking buffer overnight at 4°C. Cells were immunostained with donkey anti-mouse 488-tagged Fab secondary antibody (1:1000, Jackson ImmunoResearch) for 1 hour at room temperature. Images were acquired using Olympus IX70 inverted fluorescent microscope equipped with a 60X/0.9NA objective and operated by micro-manager software [63].

2.11 Phosphotyrosine immunoblotting

ANA-1 macrophages were plated onto 35mm-diameter well and incubated for 24 hours to obtain approximately 80% confluency. Cells were serum starved with serum-free DMEM for 4 hours under 37°C, 5% CO_2 incubation. 10μL of Protein G beads (Pierce) was washed once with 1X PBS, suspended in 100μL of 1X PBS, and then 3μL of rabbit monoclonal anti-mouse MerTK or 10μL of whole mouse IgG for isotype control was added to the beads. Beads were rotated for 30 minutes at room temperature, washed twice

with 1X PBS, and re-suspended in 3mL of 10°C serum-free DMEM. After 4 hours of serum-starvation, the cells were cooled with 10°C serum-free DMEM for 15 minutes then 2mL of 10°C bead media was added to the cells. Cells were spun at 300 x g for 1 minute at 10°C and incubated at 10°C for 20 minutes. Cells were lysed with 4X Laemmeli buffer containing $1/10^{th}$ volume of β-mercaptoethanol and protease and phosphatase inhibitors (100X), vortexed for 30 seconds, boiled at 100°C for 5 minutes, and ran on 12% SDS-PAGE. Protein bands were transferred to a nitrocellulose membrane and membrane was blocked with TBST plus 5% BSA for 4 hours. The membrane was probed with mouse monoclonal anti-phosphotyrosine antibody, clone 4G10 (1:1000; Millipore) for 2 hours and anti-mouse IR-700 (1:10,000) for 1 hour. Three-15 minutes washes with TBST followed each antibody incubation step. The membrane was imaged with LI-COR Odyssey Infrared Imaging System.

M0 primary human macrophages were cultured on 6-well plates with coverslips following "Primary human macrophage cell culture" protocol. The cells were serum-starved with serum-free RPMI for 4 hours prior to the experiment. Unstimulated cells were left on ice in serum-free HEPES RPMI while EGTA-treated cells were treated with PEG media (0.045g of sucrose, 0.019g of 5mM EGTA, and 10μL of 1X PBS) for 10 minutes on ice. To stimulate cells with IgG immune complex, whole human IgG was heated at 62°C for 20 minutes, spun at 16,000 x g for 10 minutes, and then the supernatant was added to the cells (1:40 dilution in HEPES RPMI). The cells were incubated at 37°C for 30 minutes and washed with ice-cold 1X PBS. MerTK was activated by treating the cells with 1:1000 rabbit monoclonal anti-human MerTK antibody (Abcam) for 20 minutes on ice, then crosslinking with goat anti-rabbit Cy3-tagged $F(ab')_2$ (1:1000, Jackson ImmunoResearch) for 20 minutes on ice. Cells were incubated on ice for an additional 20 minutes to enhance tyrosine phosphorylation then lysed with 4X Laemmeli buffer containing $1/10^{th}$ volume of β-mercaptoethanol and protease and phosphatase inhibitors (100X). Cell lysate was ran on 12% SDS-PAGE and transferred to nitrocellulose membrane. The membrane was blocked with 5% BSA for 4 hours, probed with mouse monoclonal anti-phosphotyrosine antibody, clone 4G10 (1:1000; Millipore) for 2 hours and anti-mouse IR-700 (1:10,000, Jackson ImmunoResearch) for 1 hour. For loading control, the membrane was probed with mouse

anti-actin antibody (1:500, Developmental Studies Hybridoma Bank) and anti-mouse IR-800. Three-15 minutes washes with TBST followed each antibody incubation step. The membrane was imaged with LI-COR Odyssey Infrared Imaging System.

2.12 Phosphotyrosine immunoprecipitation

M0 primary macrophages were cultured on a one-well plate coated with 0.1% gelatin as per "Primary human macrophage cell culture" protocol (Section 2.2). Cells were serum-starved with serum-free RPMI for 4 hours prior to the experiment. Unstimulated cells were left on ice in serum-free HEPES RPMI while MerTK activated cells were treated with rabbit monoclonal anti-human MerTK at a dilution of 1:500 for 20 minutes on ice followed by goat anti-rabbit Cy3-tagged $F(ab')_2$ secondary antibody (1:500) for 20 minutes on ice. Cells were incubated for additional 20 minutes then lysed with 1mL of lysis buffer containing wash buffer (20mM Tris-HCl pH 8.0, 0.15M NaCl, 2mM EDTA, 1% Nonidet P-40, 10% glycerol, 1mM Na_3VO_4), 0.25mM phenylmethylsulfonyl fluoride, 200nM Okadaic acid, 10mM NaF, and protease and phosphatase inhibitor (100X). The cell lysate was rotated at 4°C for 40 minutes then spun at maximum speed for 15 minutes. The supernatant was recovered and 50µL was kept for lysate controls while 40µL of anti-phosphotyrosine antibody, clone 4G10, agarose conjugate (EMD Millpore) was added to the remainder of the supernatant. The supernatant was incubated at 4°C rotating for 16 hours.

After the 16-hours incubation, the slurry was washed five times with wash buffer followed by elution with 70µL of 1X phenyl phosphate, disodium salt dehydrate (Fisher Scientific) at 4°C for 30 minutes. The slurry was spun at 4°C at maximum speed for 15 minutes and the immunoprecipitate recovered. A one-quarter volume of 4X Laemmli buffer with 50mM DTT was added to the immunoprecipitate and 0.5% total cell lysate samples, which were then boiled for 2 minutes at 100°C, and ran on a 10% SDS-PAGE at 100V for 2 hours. The gel was fixed with 40% ethanol + 10% acetic acid for 15 minutes, and stained with BioRad QC colloidal coomassie stain for 20 hours. The gel was destained with deionized water for 3 hours then imaged on Gel Doc EZ Imager from BioRad.

2.13 Quantification of mean fluorescence intensity and co-localization

Mean Fluorescence Intensity (MFI) was measured by tracing the area occupied by cells on Fiji ImageJ software while taking background measurement for each cell. Twenty cells per condition for each experiment were analyzed. Corrected means were calculated on Microsoft Excel spreadsheet by subtracting the means from the background measurements, then MFI graph was created using GraphPad Prism software.

Pearson's correlation coefficient was calculated on Fiji ImageJ software using Just Another Co-localization Plugin [64]. Thresholds values were set for 4G10 and MerTK images. R values calculated by the plugin were imported into Microsoft Excel spreadsheet which was used to calculate average R values for each group in each experiment. Calculation of standard error of the mean (SEM), graphs and statistics were then created using GraphPad Prism software.

2.14 Statistical analysis

One-tailed Student's t-tests or ANOVA using Bonferroni method were performed as appropriate using GraphPad Prism software. Data are presented as mean + SEM.

Chapter 3: Results

Chapter 3: Results

3.1 Murine macrophage cell lines lack consistent MerTK expression

Cell lines consistently expressing endogenous MerTK were required for my research. Therefore, I quantified MerTK expression using western blotting of the commonly used murine macrophage cell lines, RAW647.2 (RAW) and J774.1 [65–67]. The first western blot did not show protein band corresponding to MerTK for RAW cells but, consistent with reports in the literature [68], showed a faint band between 100-150 kDa corresponding to MerTK for J774.1 cells as indicated by the red arrow (Figure 3A). The same culture of cells displayed a plasmalamellar (ring-like) distribution of MerTK on J774.1 cell surface by confocal microscopy (Figure 3B), consistent with the J774.1 cell line expressing MerTK. However, it was not possible to consistently reproduce these results in J774.1 cells. Subsequent immunoblots either lacked any protein bands or displayed only non-specific antibody binding to proteins of the incorrect molecular mass, while subsequent microscopy experiments observed a small percentage (less than 5%) of J774.1 cells showing a weak plasmalamellar staining pattern with the bulk of the cells in the samples showing no staining (data not shown). Several alternate primary antibodies and cell culture conditions were tested, but none of these produced consistent and clear MerTK expression, thereby eliminating J774.1 cells as a viable model system.

The less commonly used ANA-1 murine macrophage cell line was then tested for endogenous MerTK expression. Both conventional immunofluorescence images (Figure 3C) and confocal microscope images (Figure 3D) revealed non-specific background fluorescence instead of the expected plasmalamellar staining indicative of MerTK expression. Since microscopy has limited sensitivity, I indirectly tested for MerTK expression by adding MerTK antibody-conjugated beads, followed by phosphotyrosine immunoblotting to detect any resulting MerTK signalling. This method was used because it has been shown that receptor activation leads to phosphorylation of downstream proteins detectable by immunoblotting [19]. The resulting immunoblot revealed only basal

Figure 3: Murine macrophage cell lines lack consistent MerTK expression.

A) Western blotting performed on RAW264.7 and J774.1 cell lysates revealed MerTK protein band only in J774.1 (red arrow). This blot represents the one experiment, out of five, which showed MerTK protein band. **B)** Fluorescent microscopy of endogenous MerTK expression on J774.1 macrophages using confocal microscopy. The image is representative of ten images captured in one experiment. Scale bar is 10 μm. **C)** Widefield microscopy image of ANA-1 macrophages immunostained with anti-mouse MerTK (red) and counterstained with DAPI (blue). Image is representative of three independent experiments. Scale bar is 10μm. **D)** Confocal Z-stack image of ANA-1 macrophage stained with anti-mouse MerTK (red). Image is representative of three images captured in one experiment. **E)** Phosphotyrosine (4G10) immunoblot of either 20μL or 40μL of ANA-1 cell lysates from non-crosslinked (Iso) or MerTK (Mer) crosslinked cells. The blot is representative of two experiments.

A)

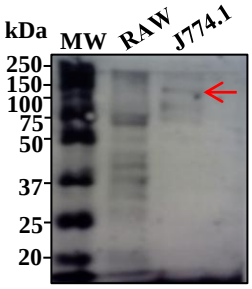
kDa
MW
RAW
J774.1
250
150
100
75
50
37
25
20

B)

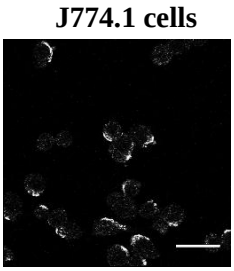
J774.1 cells

C)

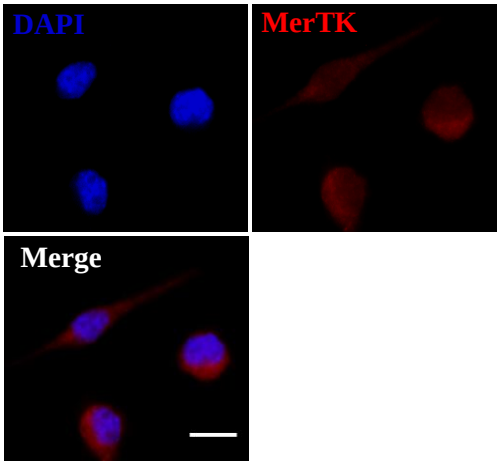
DAPI
MerTK
Merge

D)

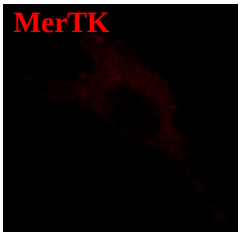
MerTK

E)

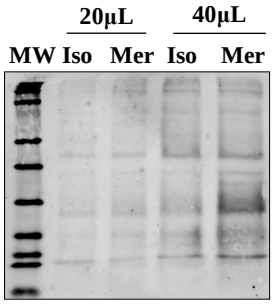
20µL
40µL
MW Iso Mer Iso Mer

levels of phosphorylation in the MerTK crosslinked lane (Figure 3E). The lack of increased phosphorylation in stimulated ANA-1 cells combined with the immunofluorescence results confirms that these cells do not express endogenous MerTK. Therefore, none of the tested murine macrophage cell lines were viable models for MerTK analysis.

3.2 Generating MerTK ectopic expression system

The lack of consistent MerTK expression on murine macrophage cell lines necessitated the generation of macrophages stably expressing ectopic MerTK. I tried several methods to clone full-length MerTK for instance, conventional cloning of wild-type human and murine MerTK, and murine GFP-tagged MerTK into the mammalian expression vector, pEGFP-N1 (Table 1, appendix Figure A1). However, screening for positive clones by restriction enzyme digestion revealed either empty vectors or inserts only a few hundred base-pairs in size (data not shown), rather than the expected 3 kb full-length MerTK amplicon produced by PCR.

Since conventional cloning methods were unsuccessful, a different approach was carried out, as highlighted in Figure 4A, to generate HA-tagged human MerTK. A SalI site was inserted into the middle of MerTK by site-directed mutagenesis in fashion that does not introduce a change in the amino acid sequence (Figure 4A). A BglII site was inserted upstream of the gene and an XhoI site downstream (Table 2). The 5’ (BglII to SalI) fragment of MerTK was amplified by PCR and cloned into the HA-containing pDisplay-LAP2 vector, while the 3’ fragment (SalI to XhoI) was to be cloned into pBluescript. Cloning of both fragments was determined to be successful by colony PCR and DNA sequencing (data not shown), after which the 3’ MerTK fragment was excised from pBluescript and ligated into the 5’ pDisplay-LAP2 vector digested with SalI and XhoI. The transformation of this construct led to recovery of only a small number of clones.

Colony PCR of the resulting constructs revealed a 3 kb band believed to be full-length MerTK (red box, Figure 4B). However, when sequenced, only MerTK constructs containing point mutations, insertion and deletions, or frame-shift mutations were

Figure 4: Generating HA-tagged human MerTK ectopic expression system.

A) SnapGene schematic of one of several strategies used to attempt cloning HA-tagged human MerTK into pDisplay-LAP2. **B)** Colony PCR gel of full-length MerTK cloned into pDisplay-LAP2. Colony 2 (red square) appears to be a full-length (3 kb) MerTK clone. **C)** Alignment comparing human MerTK with the sequence of colony 2 (C2) from panel B. Point mutations are highlighted in green, frame-shift mutation is highlighted in red, and a stop codon arising due to the frame-shift mutation is highlighted in cyan.

A)

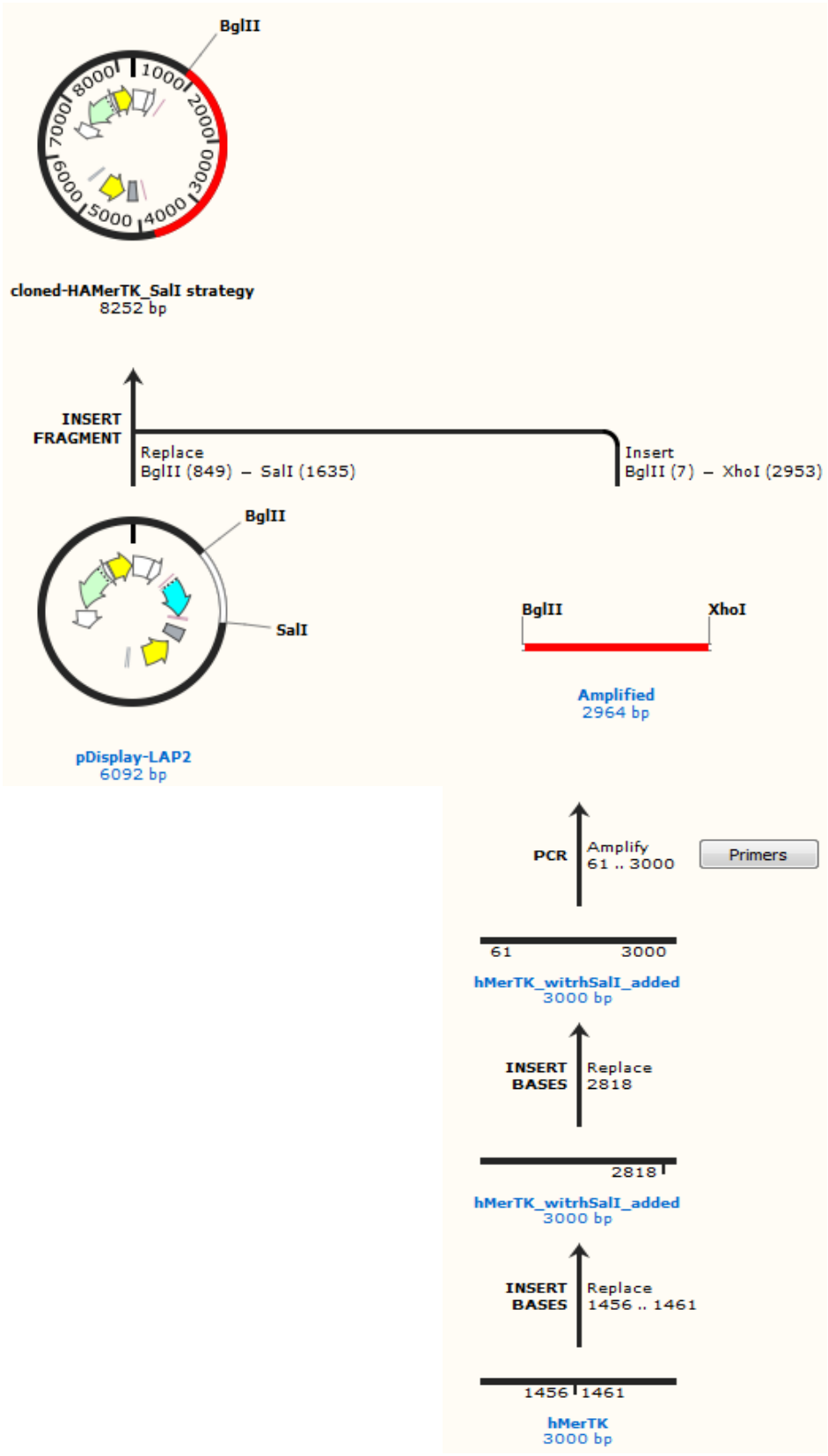
BglII
1000
2000
3000
4000
5000
6000
7000
8000
cloned-HAMerTK_SalI strategy
8252 bp
INSERT FRAGMENT
Replace
BglII (849) – SalI (1635)
Insert
BglII (7) – XhoI (2953)
BglII
SalI
pDisplay-LAP2
6092 bp
BglII
XhoI
Amplified
2964 bp
PCR
Amplify
61 .. 3000
Primers
61
3000
hMerTK_witrhSalI_added
3000 bp
INSERT BASES
Replace
2818
2818
hMerTK_witrhSalI_added
3000 bp
INSERT BASES
Replace
1456 .. 1461
1456
1461
hMerTK
3000 bp

B)

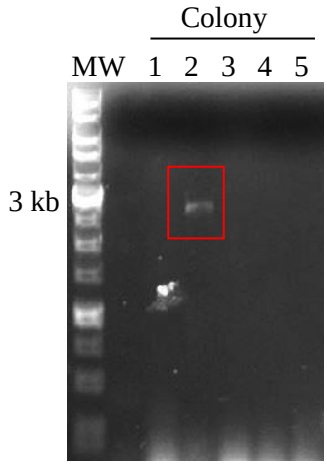

C)

```
          830        840         850         860         870
MerTK  AGTGCAGATCAACATCAAAGCAATTCCCTCCCC-ACCAACTGAAGTCAGCATCCGTAACA
       :::::::::::::::::::::: : :::::::: :::::::::::::::::::::::::
C2     AGTGCAGATCAACATCAAAGCATTCCCCTCCCCCACCAACTGAAGTCAGCATCCGTAACA

      880        890         900         910         920         930
MerTK  GCACTGCACACAGCATTCTGATCTCCTGGGTTCCTGGTTTTGATGGATACTCCCCGTTCA
       ::::::::::::::::::::::::::::::::::::::::::::::::::::::::::::
C2     GCACTGCACACAGCATTCTGATCTCCTGGGTTCCTGGTTTTGATGGATACTCCCCGTTCA
```

recovered. An example of this is shown in Figure 4C, where the alignment of a recovered MerTK clone with the reference human MerTK sequence shows both point mutations and a frame-shift mutation (highlighted in green and red, respectively). The frame-shift mutation creates a premature stop codon within the reading frame (cyan highlight, Figure 4C) producing a truncated protein lacking the transmembrane and intracellular kinase domains. The failure of our earlier cloning attempts and this sequencing result is consistent with this gene being somehow toxic to the bacteria used for cloning, perhaps due to low-level expression resulting in cytosolic expression and aggregate formation of a normally transmembrane protein. Thus, this toxicity would lead to recovery of only rare mutated sequences such as those illustrated in Figure 4C which eliminate the portions of the MerTK gene causing toxicity in the cloning bacteria.

3.3 pIRES2-EGFP murine MerTK is not expressed in transfected HeLa and RAW264.7 cells

During our attempts at cloning MerTK, a murine MerTK plasmid with MerTK under control of a mammalian promoter plus a downstream pIRES2-EGFP became available from Addgene (appendix Figure A1). I attempted to use this construct to make a stable MerTK expressing cell line that could then be used for studying MerTK signalling pathway. HeLa and RAW cells were co-transfected with this construct, plus a mCherry (example, mCherry-Rab7) expressing plasmid as a positive control for transfection. The images revealed high rates of transfection, as indicated by high levels of mCherry expression in a large proportion of both HeLa (>70% transfection) and RAW cells (>30% transfection, Figure 5, top images). However, the mCherry positive cells lacked GFP expression (Figure 5, bottom images), and thus lacked MerTK expression. Several different transfection ratios of MerTK:mCherry were tested with none producing measurable MerTK/GFP expression (data not shown). It is unclear why we did not observe MerTK/GFP expression in these cells, as sequencing of the plasmid revealed the expected sequence of MerTK and there were no signs of toxicity in the transfected cells.

Figure 5: pIRES2-EGFP murine MerTK is not expressed in transfected HeLa or RAW264.7 cells.

HeLa and RAW264.7 cells were co-transfected with mCherry-Rab7 (top images) and pIRES2-EGFP murine MerTK plasmid (bottom images). Images were taken through 60X objective on an inverted fluorescence microscope and are representative of three separate experiments. Scale bar is 10 μm.

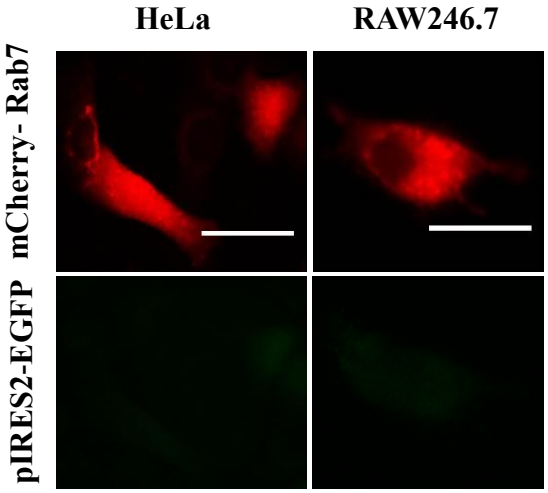
HeLa
RAW246.7
mCherry- Rab7
pIRES2-EGFP

3.4 MerTK is expressed in M0 and M2 primary human macrophages

Since none of the tested murine cell lines expressed MerTK and our attempts at cloning and expressing recombinant MerTK had failed, I altered my approach in order to use primary human cells expressing endogenous MerTK. This required identification of a phagocytic cell type that expressed MerTK under normal conditions. Therefore, I tested primary human macrophages differentiated into M0 (unpolarized), M1, or M2 subtypes and analysed them for endogenous MerTK expression.

M0 and M2 macrophages exhibited a pattern of MerTK expression characteristic of a plasma membrane localized protein, while M1 macrophages displayed mostly non-specific background fluorescence (Figure 6A). Quantification of these images revealed that 88 percent of M0 macrophages were MerTK positive, 93 percent of M2 were MerTK positive, while only 18 percent of M1 were MerTK positive (Figure 6B). When MerTK expression levels were quantified, the small portion of MerTK positive M1 cells expressed significantly less MerTK than M0 or M2 cells, while M0 and M2 cells expressed equivalent amounts of MerTK (Figure 6C). This led to the conclusion that MerTK is expressed on primary human macrophages of the M0 and M2 lineages. I chose to use M0 macrophages for all subsequent experiments as these macrophages are the least differentiated and are capable of further differentiation, thereby increasing the likelihood that results observed in these macrophages will be consistent between multiple subtypes of macrophages and will provide the opportunity to assess the impact of MerTK signalling in mediating further macrophage differentiation.

Figure 6: MerTK is expressed in M0 and M2 primary human macrophages.

A) M0, M1, and M2 macrophages were labelled with rabbit anti-human MerTK plus Dylight 488-tagged Fab (green) and DAPI (blue). Images were captured through 60X objective and are representative fields from two different experiments. Scale bar is 10 μm. **B)** Percentage of MerTK positive cells. Asterisks indicate statistically significant difference ($P < 0.05$) compared with M1 macrophages using ANOVA with Bonferonni correction. **C)** MerTK expression levels in mean fluorescence intensity. *n.s.* indicates non-significant difference between M0 and M2, and asterisk indicates significant difference compared to both M0 and M2 using ANOVA with Bonferonni correction. Twenty cells per condition per experiment were analysed. Data are shown as mean + SEM.

A)

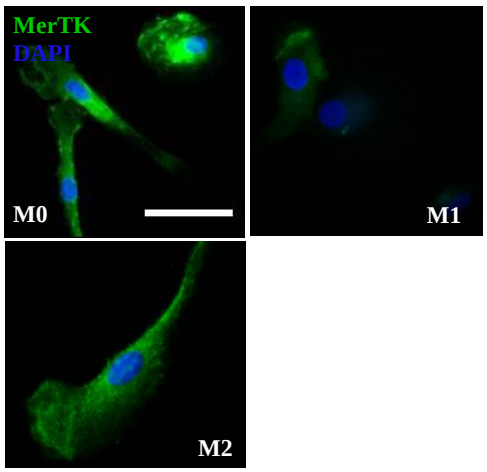
MerTK
DAPI
M0
M1
M2

B)

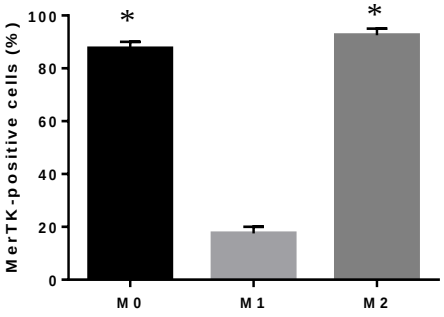
MerTK-positive cells (%)
100
80
60
40
20
0
*
*
M0
M1
M2

C)

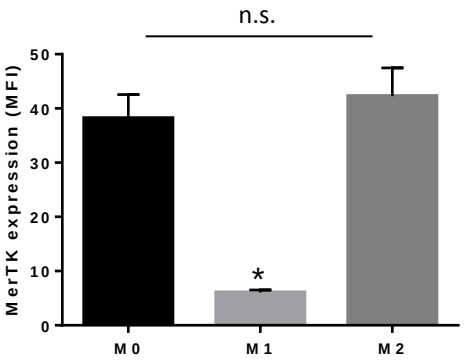
n.s.
MerTK expression (MFI)
50
40
30
20
10
0
*
M0
M1
M2

3.5 Measuring MerTK-dependent efferocytosis by M0 primary human macrophages

After it was established that MerTK is expressed on M0 macrophages, MerTK's efferocytic ability was assessed using antibody-coated beads that were expected to selectively engage MerTK, but not other efferocytic or phagocytic receptors. Different methods were used to generate these beads, with all methods aimed at masking the Fc region of the anti-MerTK antibody in order to avoid engagement of Fcγ receptors (methods used to produce the different beads is described in section 2.7). All of the various anti-MerTK-coated beads were readily internalized as indicated by the white arrows (Figures 7A left image; Figure 7B top panels).

Unfortunately, in all cases, isotype antibody-coated beads (negative controls) were internalized equally well (Figures 7A right image; Figure 7B bottom panels, white arrows), indicating that our bead preparation methods were unable to mask the Fc region of the anti-MerTK antibody, thus leading to internalization at least partially by FcγR-mediated phagocytosis. Therefore, MerTK-specific efferocytosis by M0 macrophages was not achieved, requiring that we improve the specificity of our bead model. This work is currently being pursued by other members of our laboratory.

3.6 Crosslinking MerTK on M0 primary human macrophages induces endocytosis independent of Src/Syk and PI3-kinase

It is well established that crosslinking of phagocytic receptors induces the same signalling and internalization pathways as do particulate targets engaging the same receptor [69]. Since our bead-based efferocytic assays were non-specific, we took advantage of this phenomenon and used MerTK-crosslinking to selectively stimulate MerTK on M0 primary human macrophages. MerTK was crosslinked through addition of the anti-MerTK antibody which was then either crosslinked by the addition of a Cy3-labelled dimeric secondary $F(ab')_2$. Endocytosis was quantified by first imaging total MerTK on the cells using widefield fluorescence microscopy, followed by an acid-wash to dissociate antibodies from non-internalized MerTK, and then the cells were re-imaged to detect the

Figure 7: Measuring MerTK-dependent efferocytosis by M0 primary human macrophages.

A) Efferocytosis analysis of anti-human MerTK-coated Protein A beads (left image) and whole human IgG (isotype control)-coated Protein A beads (right image). Images are representative of two experiments. **B)** Efferocytosis assay of polystyrene beads coated with anti-human MerTK then labelled with eFluor 670 (top images). Bottom images show isotype control beads. Cells were imaged through 60X objective using a widefield fluorescent microscope. Images are representative of ten images captured over three experiments. Scale bar is 10 μm.

A)

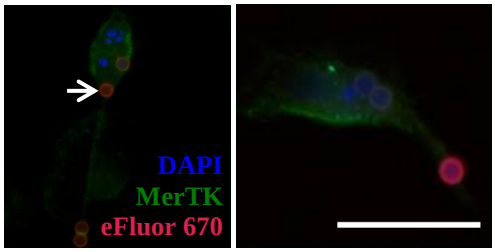
DAPI
MerTK
eFluor 670

B)

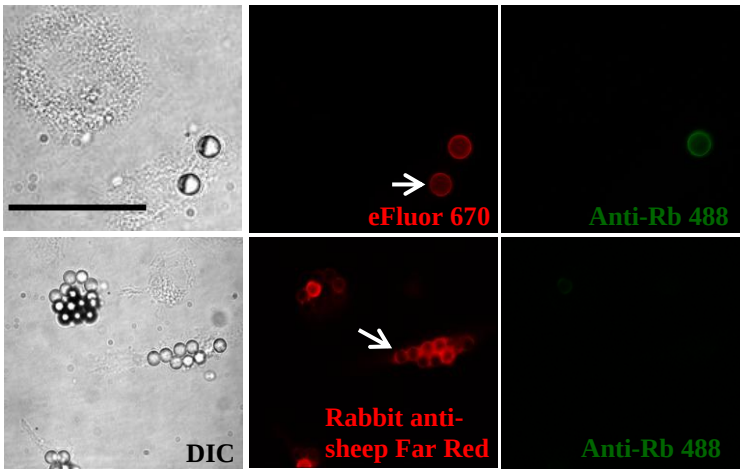
eFluor 670
Anti-Rb 488
DIC
Rabbit anti-
sheep Far Red
Anti-Rb 488

residual (internalized) MerTK signal. Endocytosis was quantified as the amount of fluorescence after acid-washing (internalized MerTK) divided by the fluorescence before acid-washing (total MerTK). These efferocytosis assays were then used to investigate the role of Src-family kinases, Syk kinase, and PI3K (all critical regulators of other phagocytic receptors) in MerTK-mediated endocytosis.

As a negative control, MerTK on M0 primary human macrophages was labelled but not crosslinked through the addition of an anti-MerTK antibody plus a monovalent Cy3-labelled secondary Fab. Without crosslinking, MerTK showed the expected plasmalamellar distribution on the surface (Figure 8A, top panel). Acid-washing removed most of this MerTK labelling (Figure 8A, bottom panel, and Figure 8C), indicating that little basal endocytosis of MerTK occurred and that Fcγ receptors were not being significantly engaged. The cells were counterstained with Cy5-WGA to demarcate their plasma membrane.

To stimulate MerTK on M0 macrophages, MerTK was activated through the addition of an anti-MerTK antibody followed by crosslinking with divalent secondary Cy3-conjugated $F(ab')_2$. As shown in the top panel of Figure 8B, crosslinking induced a punctate distribution of MerTK reminiscent of endosomes. Acid-washing was unable to remove this staining, confirming that MerTK had been internalized into an endosome-like compartment (Figure 8B, bottom panel). Quantification of cells pre- versus post-acid wash determined that 76 ± 17% of MerTK was internalized (Figure 8D).

Given that MerTK crosslinking was a viable model of MerTK internalization, I then addressed whether its endocytosis is dependent on PI3K, Syk or Src-family kinases by treating M0 primary human macrophages with inhibitors of those proteins. As before, non-crosslinked MerTK was not endocytosed (Figure 9A). When MerTK was crosslinked, endocytosis was detected even after acid-washing the cells (Figure 9B). Treatment of MerTK-crosslinked M0 macrophages with the PI3K inhibitor LY294002, the Syk inhibitor piceatannol, or the Src-family kinase inhibitor PP1, had no notable impact on MerTK endocytosis after crosslinking (Figure 9C-E). Quantification of both

Figure 8: Crosslinking MerTK on M0 primary human macrophages induces endocytosis.

MerTK endocytosis was quantified by measuring total MerTK by fluorescence microscopy, followed by removal of non-internalized MerTK staining with acid-washing and re-imaging of the samples. The plasma membrane was demarcated with Wheat Germ Agglutinin (WGA). **A)** Basal (non-crosslinked) endocytosis of MerTK. **B)** Endocytosis of crosslinked MerTK ($F(ab')_2$) on M0 macrophages **C)** Quantification of MerTK mean fluorescence intensity (MFI) of pre- versus post-acid washed, non-crosslinked condition. The asterisk indicates statistical significance by one-tailed Student's t-test ($P < 0.05$). **D)** Quantification of MerTK MFI of pre- versus post-acid washed, MerTK-crosslinked cells. *n.s* indicates no statistically significant difference between non-acid washed and acid-washed conditions; one-tailed Student's t-test. Data are presented as mean + SEM. Images are representative of three independent experiments. Scale bar is 10 μm.

A)

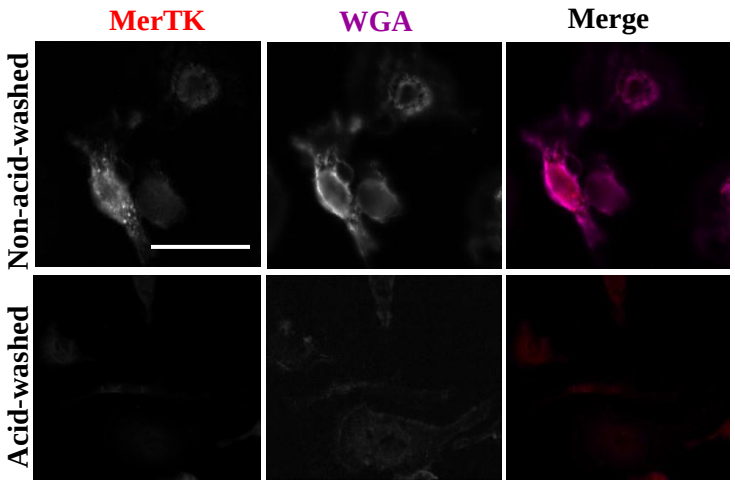
MerTK
WGA
Merge
Non-acid-washed
Acid-washed

B)

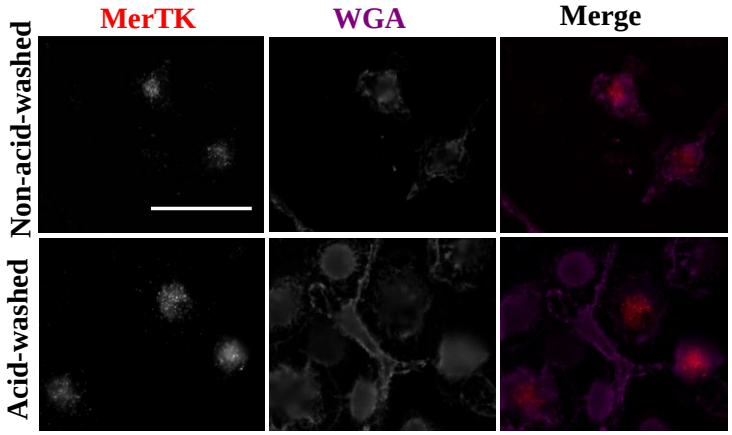
MerTK
WGA
Merge
Non-acid-washed
Acid-washed

C)

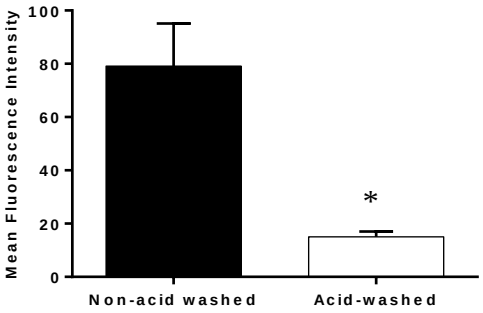
Mean Fluorescence Intensity
100
80
60
40
20
0
*
Non-acid washed
Acid-washed

D)

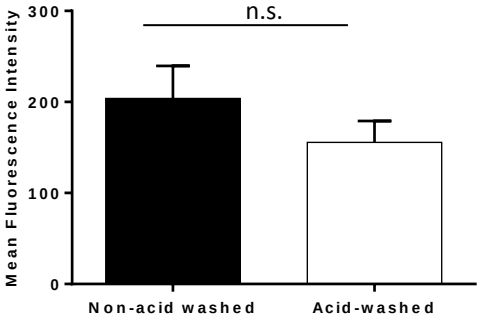
Mean Fluorescence Intensity
300
200
100
0
n.s.
Non-acid washed
Acid-washed

MerTK mean fluorescence intensity (Figure 9F) and percent internalization (Figure 9G) confirmed these results. These results demonstrate that endocytosis of MerTK is independent of PI3K, Syk, and Src-family kinases.

To confirm the effectiveness of the inhibitors, the ability of the inhibitors to block the well-established FcγR-mediated phagocytosis of IgG-coated beads was performed using RAW macrophages. RAW macrophages were fed unlabelled IgG-coated beads and after an internalization period, non-internalized beads were labelled with a Dylight 488-conjugated secondary antibody (green). As expected, untreated cells readily phagocytosed the majority of beads (Figure 10A, 10E) and FcγR-mediated phagocytosis was considerably blocked by all three inhibitors, LY294002, piceatannol, and PP1 (Figure 10B-D, 10E).

Figure 9: Endocytosis of MerTK is independent of Src/Syk-kinases and PI3K.

MerTK endocytosis was quantified by measuring total MerTK by fluorescence microscopy, followed by removal of non-internalized MerTK staining with acid-washing and re-imaging of the samples. The plasma membrane is demarcated by WGA. **A)** Endocytosis of MerTK in unstimulated (Fab labelled) M0 macrophages. **B)** Endocytosis assay of untreated MerTK-crosslinked ($F(ab')_2$) M0 macrophages. **C-E)** Endocytosis assay of PI3K-inhibited (C, LY294002), Syk-inhibited (D, piceatannol), and Src-family kinase-inhibited (E, PP1) MerTK-crosslinked macrophages. **F)** MerTK MFI pre and post acid-washing on either untreated or inhibitor-treated M0 macrophages. **G)** Percent MerTK internalization based on the data from panel F. All images are taken through 60X objective. Scale bar is 10 μm. Data are presented as mean + SEM from three independent experiments. Differences among means are not statistically significant by ANOVA with Bonferroni correction.

A)

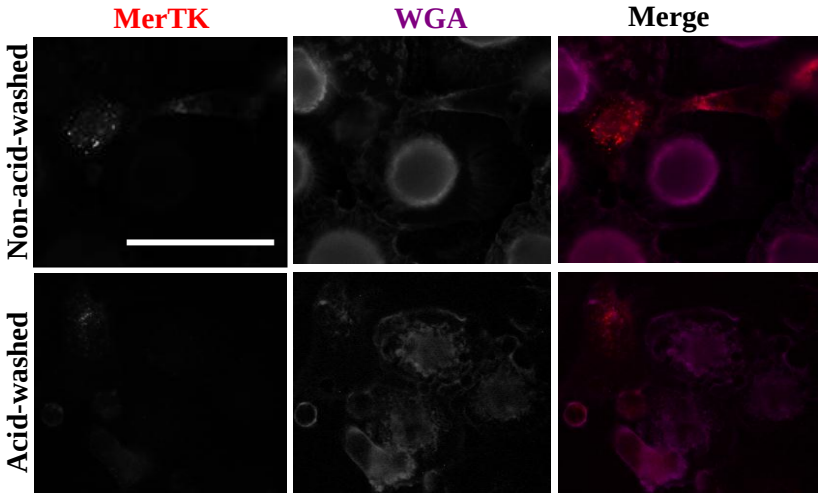
MerTK
WGA
Merge
Non-acid-washed
Acid-washed

B)

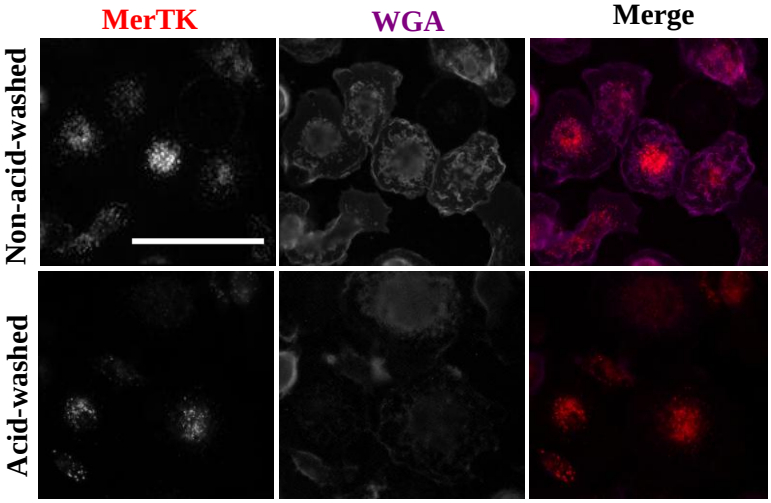
MerTK
WGA
Merge
Non-acid-washed
Acid-washed

C)

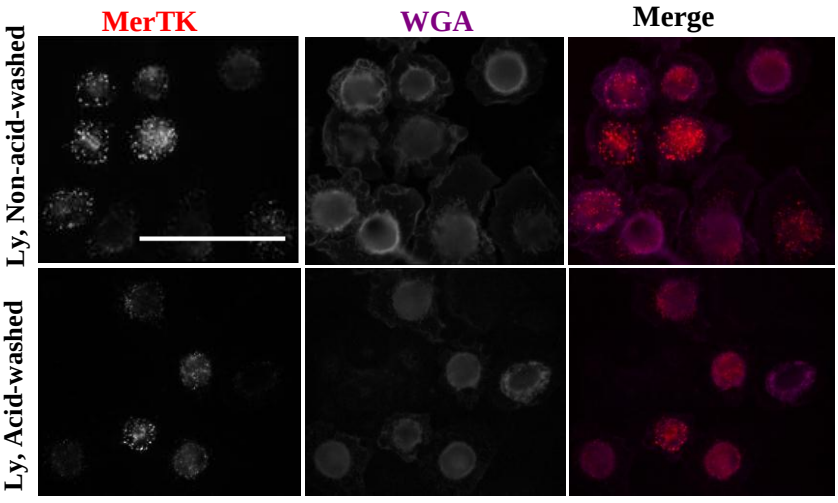
MerTK
WGA
Merge
Ly, Non-acid-washed
Ly, Acid-washed

D)

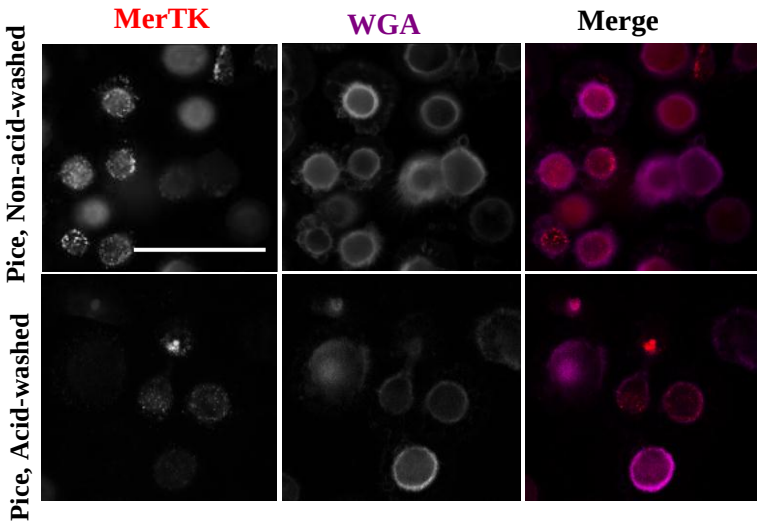
MerTK
WGA
Merge
Pice, Non-acid-washed
Pice, Acid-washed

E)

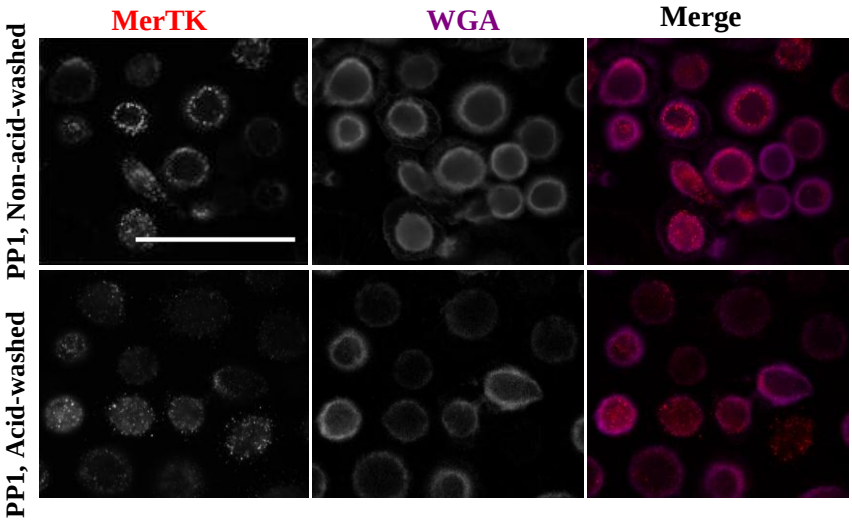
MerTK
WGA
Merge
PP1, Non-acid-washed
PP1, Acid-washed

F)

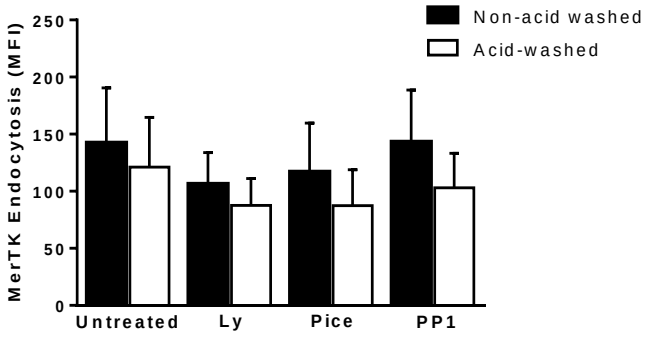
Non-acid washed
Acid-washed
MerTK Endocytosis (MFI)
250
200
150
100
50
0
Untreated
Ly
Pice
PP1

G)

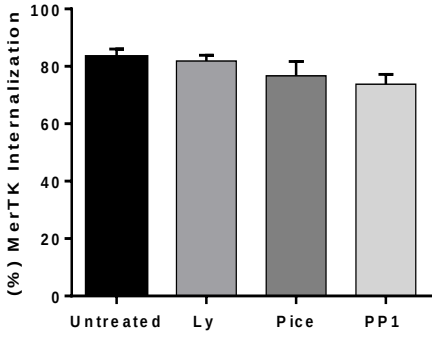
(%) MerTK Internalization
100
80
60
40
20
0
Untreated
Ly
Pice
PP1

Figure 10: Inhibition of IgG-mediated

A) DIC and 488 channel (green) images of IgG-mediated phagocytosis on untreated RAW macrophages as positive control. **B-D)** DIC and 488 channel images of IgG-mediated phagocytosis on B) PI3K, C) Syk, and D) Src-family kinase-inhibited RAW264.7 macrophages. **E)** Phagocytic index of untreated, PI3K-inhibited (LY294002), Syk-inhibited (piceatannol), and Src-family kinase-inhibited (PP1) RAW264.7 macrophages; (n = 1). Scale bar is 10 μm.

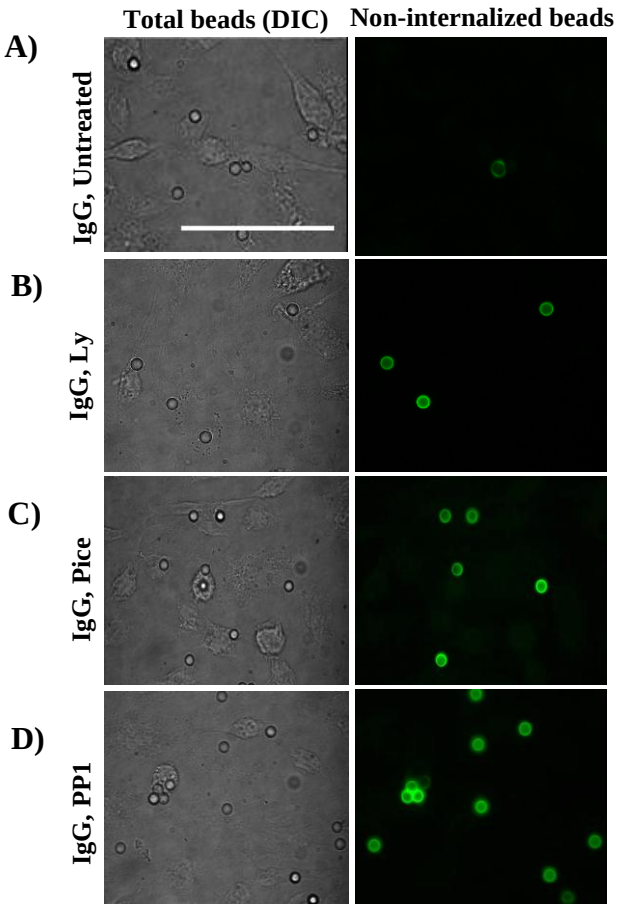
Total beads (DIC)
Non-internalized beads
A)
IgG, Untreated
B)
IgG, Ly
C)
IgG, Pice
D)
IgG, PP1

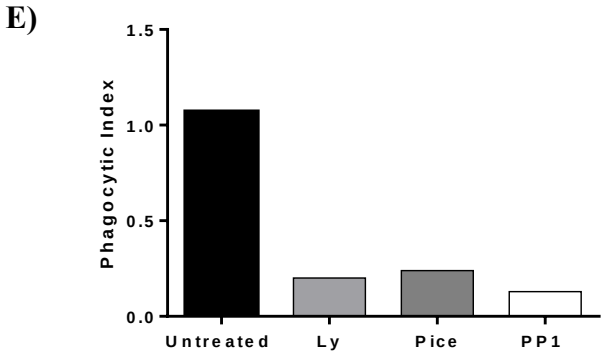
E)
Phagocytic Index
1.5
1.0
0.5
0.0
Untreated
Ly
Pice
PP1

3.7 Tyrosine phosphorylation of MerTK on M0 primary human macrophages is partially dependent on Src/Syk and PI3-kinase

Previous studies have shown that activating phagocytic receptors by crosslinking will lead to phosphorylation of the downstream proteins which drive the internalization of the phagocytic targets [69]. Our results revealed MerTK endocytosis follows crosslinking, so we investigated whether activating MerTK on M0 macrophages would also induce tyrosine phosphorylation like that observed downstream of classical phagocytic receptors. Phosphotyrosine (4G10) immunostaining of unstimulated M0 macrophages detected typical patterns and levels indicative of basal protein phosphorylation, with the phosphotyrosine immunostaining showing the punctuate staining typical of focal adhesions that account for a large portion of basal phosphorylation (Figure 11A). As a positive control we activated Fcγ receptors with aggregated IgG, which has been previously established to trigger a large increase in tyrosine phosphorylation [69], and observed the expected increase in numerous punctate phosphotyrosine structures on the cells consistent with aggregated IgG-activated Fcγ receptors (Figure 11B).

When MerTK was labelled, but not crosslinked, through the addition of anti-MerTK plus a Cy3-conjugated Fab antibody, basal levels of phosphorylation were observed (Figure 11C, top panel). Crosslinking MerTK with Cy3-conjugated $F(ab')_2$ appeared to increase total cellular tyrosine phosphorylation (Figure 11C, bottom panel). We noticed that enriched phosphotyrosine staining was only observed on cells with strong MerTK signal (white arrows), consistent with this increase in phosphorylation being due to MerTK crosslinking. To confirm these data, Pearson's co-localization analysis of MerTK with phosphotyrosine (4G10) staining was performed. The Pearson's R-value was greatly increased on MerTK crosslinked cells, indicating a strong co-localization of phosphoproteins with MerTK (Figure 11D). Despite this strong co-localization after crosslinking there was no statistically significant difference in the 4G10 mean fluorescence intensity between basal and MerTK-crosslinked condition, although the data trended towards increased phosphorylation (Figure 11E).

Figure 11: Co-localization of MerTK and tyrosine-phosphorylated proteins on M0 primary human macrophages in response to MerTK crosslinking.

A) Unstimulated M0 macrophages expressing MerTK were immunostained for tyrosine-phosphorylated proteins (4G10, green). **B)** M0 macrophages stimulated with aggregated human IgG were immunostained for tyrosine-phosphorylated proteins. **C)** MerTK on M0 macrophages were either unstimulated (Fab, top panel) or crosslinked ($F(ab')_2$, bottom panel), then the cells were immunostained to detect tyrosine-phosphorylated proteins (4G10, green). **D)** Pearson's correlation coefficient between immunostaining of MerTK and tyrosine-phosphorylated proteins (4G10) in images of unstimulated macrophages (Fab) and MerTK-crosslinked macrophages ($F(ab')_2$). The asterisk indicates $P < 0.05$ compared with Fab by one-tailed Student's t-test. Ten fields were analysed from four experiments. **E)** Fold change of tyrosine-phosphorylated protein expression of unstimulated (basal), aggregated human IgG (AgIgG), non-crosslinked MerTK (Fab), and crosslinked MerTK ($F(ab')_2$) cells. Results are representatives of four experiments (n = 4 + SEM). *n.s.* denotes no significant difference by ANOVA with Bonferroni correction. Scale bar is 10 μm.

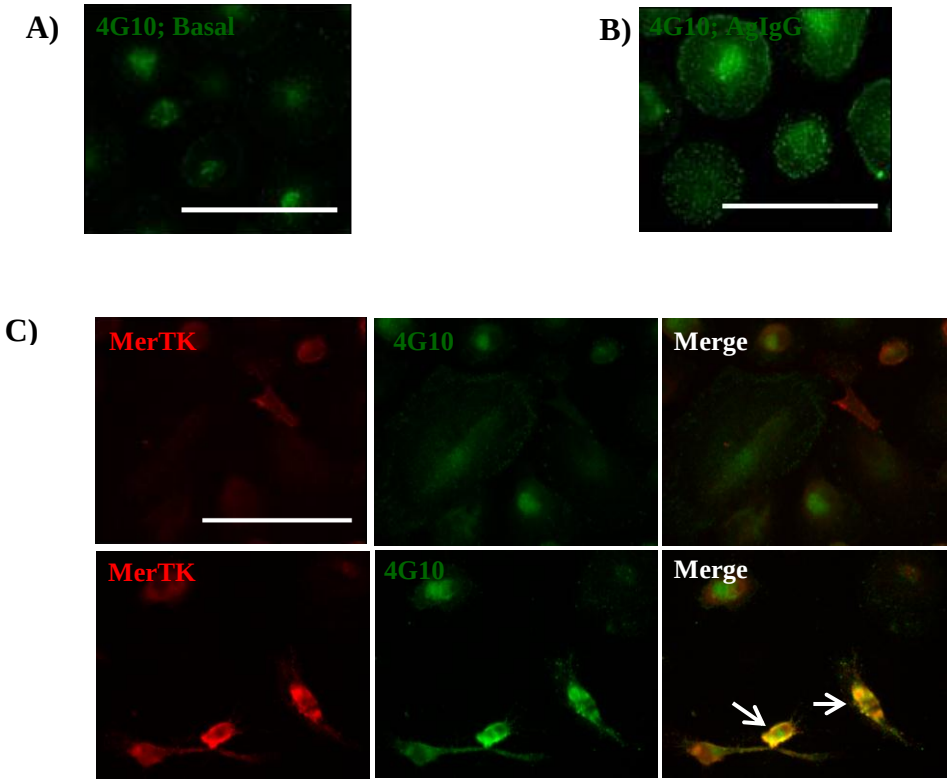
A)
4G10; Basal
B)
4G10; AgIgG
C)
MerTK
4G10
Merge
MerTK
4G10
Merge
D)
Pearson's Correlation Coefficient
1.0
0.8
0.6
0.4
0.2
0.0
*
Fab
F(ab')2
E)
Fold change relative to basal (MFI)
2.5
2.0
1.5
1.0
0.5
0.0
n.s.
n.s.
n.s.
Basal
AgIgG
Fab
MerTK x-link

Next, I assessed the impact of inhibiting PI3K, Syk, and Src-family kinases on MerTK-induced patterns of protein phosphorylation. Unstimulated or MerTK-crosslinked M0 macrophages were either left untreated or treated with the PI3K inhibitor LY294002, the Syk inhibitor piceatannol, or Src-family kinase inhibitor PP1, and then immunostained for phosphoproteins.

These inhibitors decreased the basal level of phosphorylation in unstimulated cells (Figure 12A). As expected, all three inhibitors decreased phosphorylation in response to Fcγ receptor activation of protein phosphorylation (Figure 12B). Unexpectedly, crosslinking MerTK led to increased tyrosine phosphorylation (Figure 12C) that was partially blocked by LY294002 and piceatannol (Figure 12D, E, respectively). PP1 was also inhibitory of MerTK-mediated phosphorylation (Figure 12F), consistent with the finding from Mero *et al.* [69]. Quantification of the mean fluorescence intensity confirmed that all three inhibitors induced a statistically significant inhibition of phosphorylation in both aggregated human IgG-treated and MerTK crosslinked cells (Figure 12G). Pearson's co-localization analysis showed a similar trend, although PI3K inhibition did not reach statistical significance (Figure 12H). These results demonstrate that MerTK tyrosine phosphorylation in response to crosslinking is partially dependent on PI3K, Syk and Src-family kinases.

Figure 12: MerTK tyrosine phosphorylation in response to receptor crosslinking is partially dependent on Src/Syk-kinases and PI3K.

A) 4G10 immunostaining was performed on unstimulated M0 macrophages *(top-left),* or unstimulated M0 macrophages treated with a PI3K inhibitor (LY294002, *top-right),* Syk inhibitor (piceatannol, *bottom-left),* or Src-family kinase inhibitor (PP1, *bottom-right).* **B)** 4G10 immunostaining was performed on M0 macrophages stimulated with aggregated human IgG. Cells were either left untreated or treated with PI3K, Syk or Src-family kinase inhibitors. **C)** MerTK on untreated M0 macrophages was activated with Cy3-tagged $F(ab')_2$ antibody then cells were immunostained for phosphotyrosine. **D-F)** MerTK on D) PI3K-inhibited (LY294002), E) Syk-inhibited (piceatannol) or F) Src-family kinase-inhibited (PP1) M0 macrophages was crosslinked using a Cy3-tagged $F(ab')_2$ antibody (red) and the cells were immunostained for phosphotyrosine (4G10). **G)** Phosphotyrosine MFI of basal, aggregated human IgG, and MerTK-crosslinked ($F(ab')_2$) cells either left untreated or treated with inhibitors. Data are means + SEM for each condition, from two experiments. **H)** Pearson's correlation coefficient was measured between MerTK and phosphotyrosine on MerTK-crosslinked M0 macrophages that were either uninhibited or treated with inhibitors for PI3K, Src-family kinase or Syk. *n.s.* indicate non-statistically significant decrease in co-localization of MerTK with 4G10. Asterisks indicate statistically significant changes ($P < 0.05$) by ANOVA with Bonferroni correction. Scale bar is 10 μm.

A)

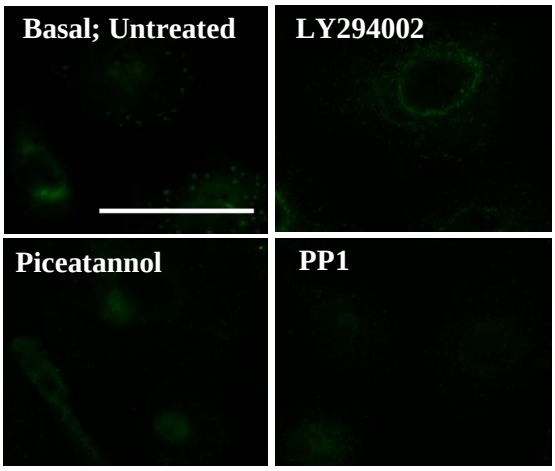
Basal; Untreated
LY294002
Piceatannol
PP1

B)

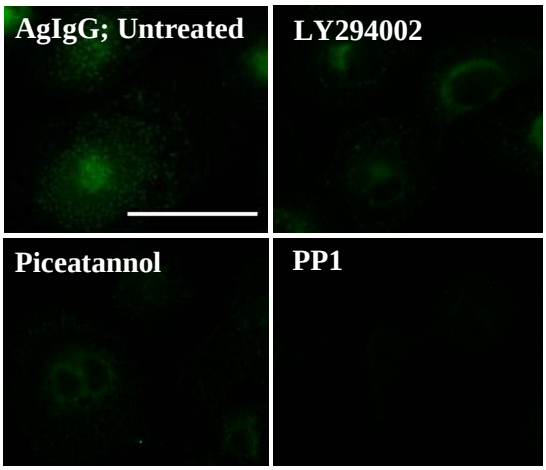
AgIgG; Untreated
LY294002
Piceatannol
PP1

C)

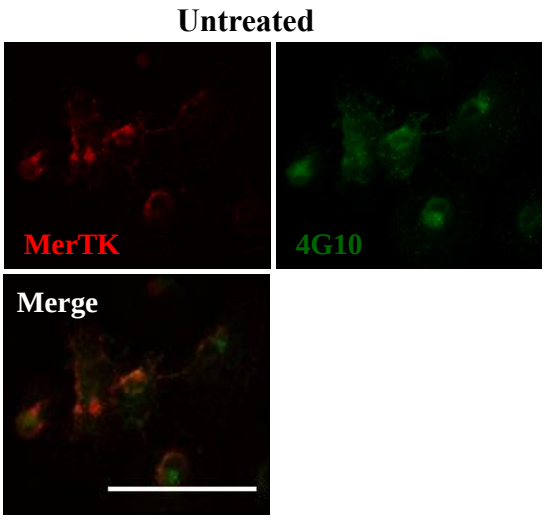
Untreated
MerTK
4G10
Merge

D)

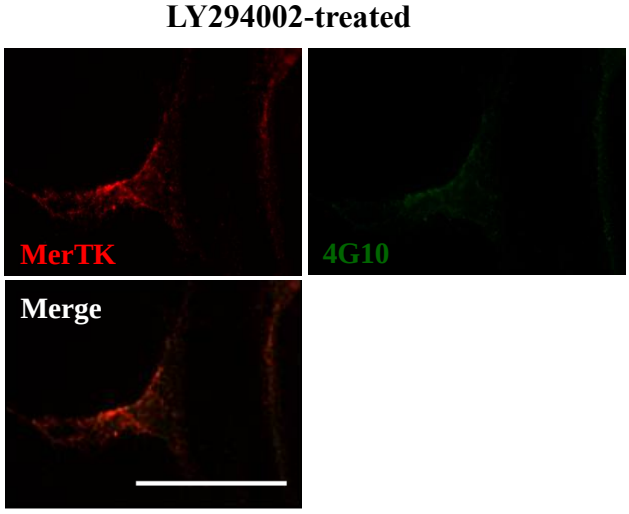
LY294002-treated
MerTK
4G10
Merge

E)

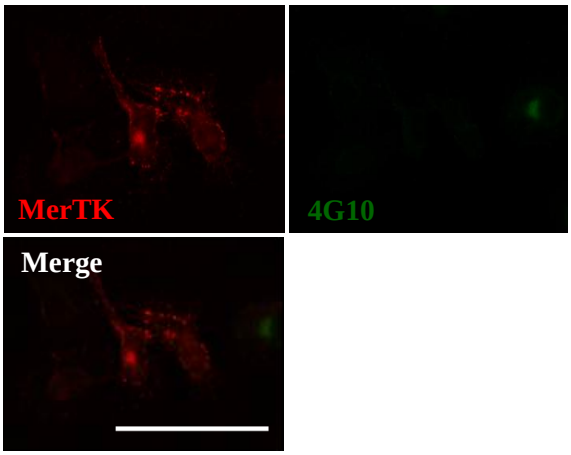
Piceatannol-treated
MerTK
4G10
Merge

F)

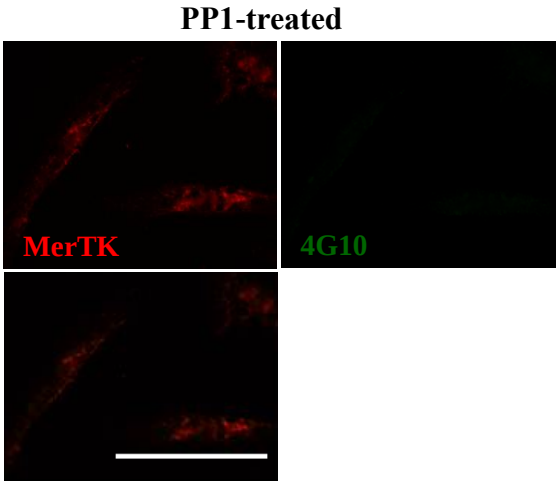
PP1-treated
MerTK
4G10

G)

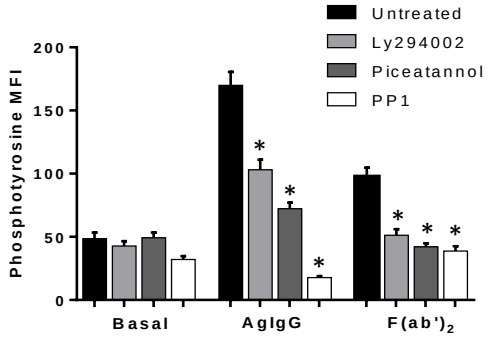
Untreated
Ly294002
Piceatannol
PP1
Phosphotyrosine MFI
200
150
100
50
0
*
*
*
*
*
*
Basal
AgIgG
F(ab')2

H)

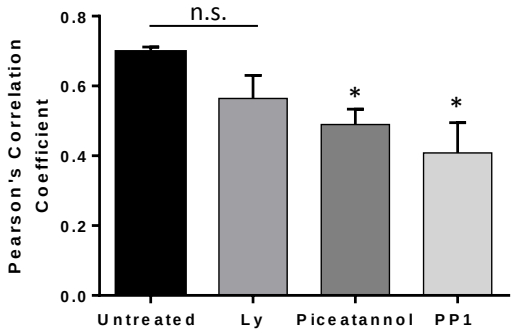
n.s.
Pearson's Correlation Coefficient
0.8
0.6
0.4
0.2
0.0
*
*
Untreated
Ly
Piceatannol
PP1

3.8 Crosslinking MerTK on M0 primary human macrophages promotes tyrosine phosphorylation

Immunoblotting was used to further investigate MerTK-mediated protein phosphorylation. Cell lysates from M0 macrophages that were either unstimulated, depleted of focal contact phosphorylation by EGTA treatment, treated with aggregated human IgG as a positive control, or MerTK-crosslinked, were separated by SDS-PAGE and immunoblotted for tyrosine-phosphorylated proteins. Increased tyrosine phosphorylation was noted when MerTK was crosslinked (Figure 13), although it was much smaller in magnitude and impacted a small number of proteins than did aggregated human IgG-induced phosphorylation. Moreover, a phosphoband at approximately 125 kDa corresponding to MerTK was apparent on the immunoblot (Figure 13, arrow), suggestive of MerTK autophosphorylation. This led us to conclude that crosslinking MerTK induces phosphorylation of a small subset of downstream proteins.

3.9 Activation of MerTK on M0 macrophages followed by immunoprecipitation of phosphorylated proteins

Next, I wanted to identify the proteins being phosphorylated in response to MerTK crosslinking through immunoprecipitation and mass spectrometry. M0 macrophages were either left unstimulated or MerTK was crosslinked, then cell lysates were incubated with 4G10 (anti-phosphotyrosine) conjugated agarose beads followed by elution of the proteins, separation on SDS-PAGE and detection by coomassie staining. Despite several attempts and multiple troubleshooting steps, we were unable to recover phosphoproteins from these cell lysates (Figure 14). I suspect this failure to recover phosphoproteins was likely due to a combination of the low expression of MerTK (relative to other receptors such as FcγRIIA), which in turn produced a weak induction protein phosphorylation after crosslinking. This was further aggravated by the limited number of macrophages we can produce from a single blood preparation. Consequently, we are reattempting the cloning of MerTK to create a cell line which expresses higher levels of MerTK, in the hopes that such a cell line would produce a higher level of MerTK-dependent phosphorylation and thus provide a viable model for the purification of phosphoproteins.

Figure 13: Crosslinking MerTK on M0 primary human macrophages promotes tyrosine phosphorylation.

Phosphotyrosine (4G10) immunoblot of cell lysates from basal, EGTA-treated, aggregated human IgG (AgIgG)-treated, and MerTK crosslinked (MerTK x-link) M0 macrophages. Arrow indicates a phosphoband of the same molecular mass as MerTK. Actin was immunoblotted (below) to ensure equal loading. Blot is representative of four similar experiments.

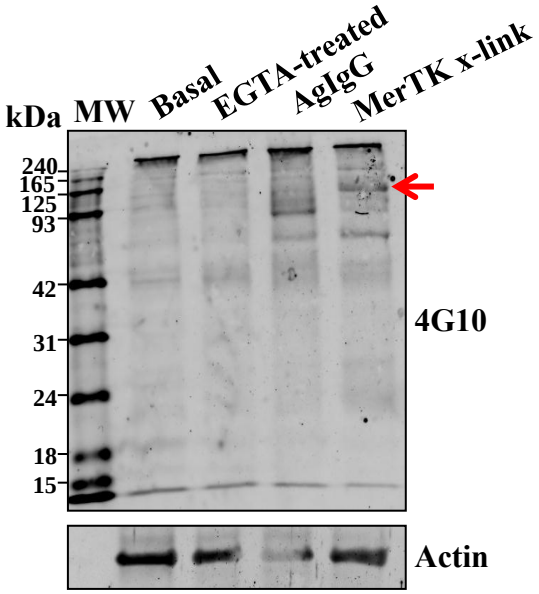
kDa
MW
Basal
EGTA-treated
AgIgG
MerTK x-link
240
165
125
93
42
31
24
18
15
4G10
Actin

Figure 14: Activation of MerTK and immunoprecipitation of tyrosine-phosphorylated proteins.

Phosphotyrosine immunoprecipitates (pY IP) were prepared from unstimulated (basal) or MerTK-crosslinked (MerTK x-link) M0 primary human macrophages. The gel shown is representative of six similar experiments.

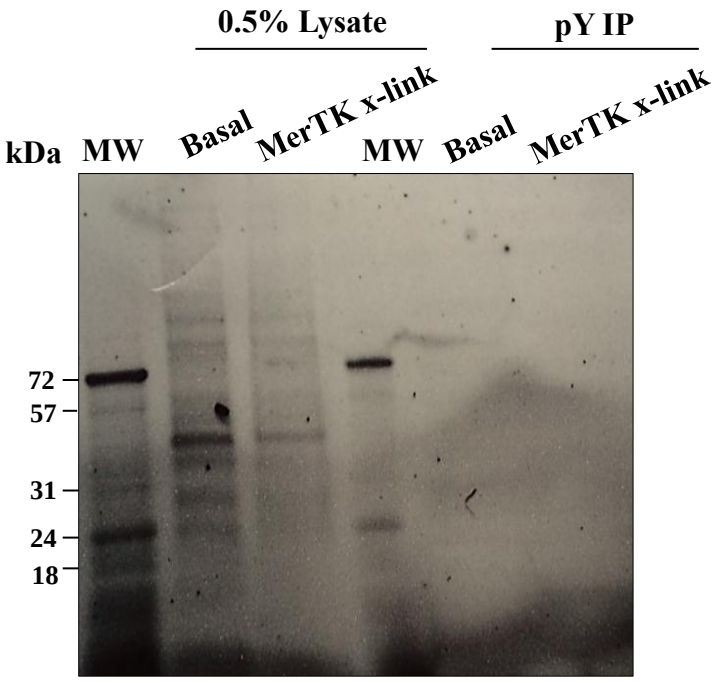
0.5% Lysate
pY IP
kDa
MW
Basal
MerTK x-link
MW
Basal
MerTK x-link
72
57
31
24
18

When successful, this model will be used to identify proteins phosphorylated in response to MerTK ligation through immunoprecipitation of the phosphorylated proteins, followed by identification by mass spectrometry.

Chapter 4: Discussion

Chapter 4: Discussion

4.1 MerTK signalling in efferocytosis

Efferocytosis is important for the maintenance of cellular homeostasis as it prevents autoimmunity and inflammation caused by the release of alarmins and autoantigens from uncleared apoptotic cells. MerTK is a major efferocytic receptor and studies have shown that MerTK mutations impair efferocytosis, leading to accumulation of apoptotic cells and the subsequent pathogenic release of alarmins and autoantigens through secondary necrosis [34,35,41]. The importance of MerTK was first identified in the retina, where MerTK is vital for proper clearance of shed photoreceptor outer segments by retinal pigment epithelial (RPE) cells. This discovery was made in the RCS rat model which has a recessively inherited retinal degeneration caused by a mutation in the MerTK gene [35,70]. Similar mutations are found in individuals with retinitis pigmentosa, further highlighting the importance of MerTK in maintenance of the retina [37].

MerTK plays a similarly important role in other tissues, but it should be noted that the importance of MerTK relative to other efferocytic receptors varies between tissues. For example, the accumulation of apoptotic cardiomyocytes is not impaired in MerTK deficient animals as there are other efferocytic receptors that compensate for the absence of MerTK [71]. However, defective MerTK signalling in mice bone marrow macrophages has been shown to promote accumulation of apoptotic cells in models of atherosclerosis, leading to inflammation-accelerated atherosclerosis [42]. For example, in a study by Thorp *et al.* [43], in a mouse model of atherosclerosis, MerTK mutation reduced clearance of apoptotic cells and promoted necrosis within the atherosclerotic plaque. In other models, MerTK has been found to be crucial for prevention of autoimmunity. In particular, MerTK mutations and the resulting failure to clear apoptotic cells produces an SLE-like disease driven by impaired efferocytosis [40]. MerTK signalling is critical to prevent this pathology, as mice lacking only the intracellular kinase domain of MerTK also develop lupus-like autoimmunity [3].

Little is known of MerTK's signalling pathway; with all signalling discovered to date elucidated using the RPE phagocytosis model. Shelby *et al.* [26] evaluated MerTK

interactions with SH2-domain containing proteins and detected MerTK interactions with Grb2, Vav3, PIK3R1, and Src. Src activation was detected downstream of MerTK and siRNA knockdown of Grb2 impaired efferocytosis of photoreceptor outer segment. Their findings suggest that SH2-domain proteins are integral part of MerTK signalling in RPE, but also account for all of what is known of MerTK signalling in the context of efferocytosis.

I hypothesized that MerTK signalling occurs through a pathway unique from that utilized by conventional phagocytic receptors such as FcγR and $\alpha_m\beta_2$. The rational for this hypothesis was two-fold, namely 1) other studies have not identified a role for the proteins normally involved in these phagocytic pathways downstream of MerTK, and 2) MerTK signalling and the resulting efferocytosis is immunologically silent, while conventional phagocytosis is pro-inflammatory and immunogenic. Both of these findings strongly suggest that MerTK is not signalling through the same signalling pathways used by conventional phagocytic receptors.

4.2 MerTK expression

MerTK expression had previously been reported in J774.1 murine macrophages [68], but we were unable to observe consistent MerTK expression in this cell line despite using multiple detection techniques and culture conditions. This inconsistency in expression suggest that MerTK expression is regulated by unknown cell culture conditions such as cell density or the levels of particular cytokines within the fetal bovine serum used to prepare the culture media. RAW264.7 and ANA-1 murine macrophages were not found to express MerTK, nor could signalling in response to MerTK crosslinking be detected in ANA-1 cells (Figure 3E). Other studies have suggested that these murine cell lines are constitutively differentiated into an M1 macrophage phenotype [72], which our results indicate weakly express MerTK (Figure 6). This differentiation may also explain the poor MerTK expression in J774.1, RAW264.7 and ANA-1 cells.

Our failure to identify endogenous MerTK expression in murine cell lines necessitated the generation of ectopic MerTK-expressing cells. To date, no other studies have used an ectopic expression system of full-length MerTK like the one I attempted to develop.

Indeed, I am aware of only open study which used recombinant MerTK, and that study only used the intracellular kinase domain of the gene [71]. The lack of ectopic expression tools is probably due to the apparent toxicity of the MerTK gene to the DH5α *Escherichia coli* cells used in all of our cloning approaches. Indeed, we have only ever recovered MerTK clones mutated such that the transmembrane/intracellular portions of the protein would not be expressed (Figure 4C), consistent with these domains being toxic if expressed in *E. coli*. Consequently, our future work may attempt to clone MerTK using yeast cells (eukaryotic cells) as they are more likely to be able to support constructs expressing proteins with eukaryotic-specific motifs such as the secretion signals required for the proper localization of transmembrane domains [73].

This study then used primary human macrophages as model system for elucidating MerTK signalling. Peripheral blood mononuclear cells were differentiated into M0, M1, and M2 macrophages through culturing the cells in the presence of specific growth factors and environmental stimuli. These differentiation protocols are well-established and have been verified by flow cytometry [74,75]. M0 macrophages were generated by culturing with M-CSF and closely resembled the phenotype of macrophages resident in healthy tissues. Indeed, M0 macrophages are thought to represent the subtype of macrophages involved in tissue homeostasis [76]. M1 macrophages were generated by culturing monocytes with GM-CSF, LPS, and IFN-γ, and are considered to be classically activated, pro-inflammatory cells like those found at the sites of bacterial infections [76,77]. M2 macrophages differentiate in the presence of M-CSF plus anti-inflammatory cytokines such as IL-4, and are considered to be alternatively activated towards a phenotype that suppresses inflammation and promotes cell growth and tissue repair [76,77].

Immunofluorescence analysis was performed on differentiated macrophages to identify endogenous MerTK. I hypothesize that MerTK will be present on anti-inflammatory and homeostatic (M2 and M0) primary macrophages. As expected, MerTK labelling was observed in the M0 and M2 subtypes (Figure 6). M0 cells were used for subsequent experiments because these cells are relatively undifferentiated and retain a strong capacity for phagocytosis [76]. My results slightly conflict with the observations of Zizzo *et al.* [78], who observed MerTK expression on all subtypes of human macrophages, but with

greatly enriched MerTK expression on the anti-inflammatory M2c subtype. This subtype of M2 macrophages is formed in the presence of M-CSF and glucocorticoid steroid hormones, and represents a cell that is further differentiated compared to the M2 phenotype induced in my experiments. Indeed, I found MerTK expression on M0 macrophages as well as M2 macrophages without further differentiation into the M2a/b/c subtypes, while contrary to this study, did not observe MerTK on M1 cells. The discrepancy is likely attributable to differences in the cell differentiation methods used by us versus Zizzo *et al.* [78]. Specifically, M-CSF was used in all differentiation media used by Zizzo *et al.* [78], while we used M-CSF only in M0 and M2 cultures. This suggests that MerTK may be an M-CSF inducible gene – a possibility undergoing further investigation in our lab.

Since different *in vitro* culture methods lead to differences in MerTK expression in cells supposedly differentiated to the same subtype, it will be necessary in the future to assess MerTK in macrophages isolated from M0, M1, and M2-like *in vivo* environments. Regardless, the observed expression of MerTK on M0 and M2 macrophages in my study (Figure 6) is consistent with these cell types needing to engage in efferocytosis as a homeostatic (M0) or tissue remodelling (M2) mechanism. The absence of MerTK on M1 macrophages (Figure 6) would be consistent with wanting to avoid efferocytosis by cells actively involved in inflammation and antigen presentation.

4.3 Elucidating MerTK signalling

I first attempted to elucidate MerTK signalling using beads that would selectively engage MerTK in a manner that mimics the particulate nature of apoptotic bodies. Challenges were encountered while assessing the efferocytic ability of MerTK using this antibody-coated bead model as I was unable to selectively engage MerTK without co-stimulating Fcγ receptors on the macrophages (Figure 7). Such a bead-based model is preferable to crosslinking assays as it recapitulates the particulate nature of apoptotic cells. Indeed, studies of phagocytosis have demonstrated that while both crosslinking and bead-based assay activate the same signalling pathways, the apparent role of these pathways in internalization can be different for crosslinked receptors (example, endocytosis) versus particulate targets (phagocytosis). For example, PI3K is activated by both crosslinking

Fcγ receptors and by IgG-coated beads but is only required for the uptake of IgG-coated beads with a diameter greater than 3μm [24,51]. Even if these bead-based assays worked, they likely would have been incomplete as it may have been difficult to incorporate $\alpha_v\beta_5$-specific antibodies or ligands into this bead-based model, making it hard to assess the cooperation of MerTK with integrins [58,79].Therefore, it is critical in the future that we generate a MerTK-specific activation model involving a particulate target that incorporates both MerTK-specific and integrin-specific components.

Apoptotic cells plus exogenously-produced MerTK-specific opsonins were considered, but will not suffice as they will express a range of "eat me" signals [9,15], including some which can be engaged by receptors such as TIM-4 that are capable of directly binding to and internalizing apoptotic cells independently of any opsonins [22]. Therefore, future studies will clone the MerTK-specific opsonin, Gas-6, and the integrin-specific opsonin, MFG-E8 (lactadherin) [14]. Once they are purified, these proteins can be coated onto polystyrene beads singularly or together in order to create MerTK-specific, integrin-specific, or dually-specific efferocytotic targets. This tool would allow us to selectively engage MerTK or $\alpha_v\beta_5$ integrin alone or together, enabling a better differentiation of their function in MerTK-mediated efferocytosis and signalling pathways.

Although we were unable to create a MerTK-specific particulate target, it is well established that crosslinking phagocytic receptors induces the same signalling pathways as does a particulate target engaging the same receptor [69]. For example, the efferocytic receptor, CD36, has been shown to signal and endocytose upon crosslinking with anti-CD36 IgA and a secondary $F(ab')_2$ antibody using the same pathways required for CD36-mediated phagocytosis of pathogens, and uptake of other particulates such as oxidized LDL [19]. Similarly, we were able to induce endocytosis by crosslinking MerTK with a $F(ab')_2$. $F(ab')_2$ was used to avoid stimulating Fcγ receptors present on macrophages, which specifically recognize the Fc region of antibodies that is removed during preparation of $F(ab')_2$ fragments [19]. Using this model, we assessed the role of Src-family kinases, Syk, and PI3K on MerTK-mediated endocytosis and phosphotyrosine signalling (Figures 9, 12).

Our studies identified a significant decrease in MerTK-induced protein phosphorylation when PI3K activity was inhibited (Figure 12D). Despite this, PI3K inhibition had no impact on the endocytosis of crosslinked MerTK (Figure 9C). This is consistent with the observations of Cox *et al.* [51], who determined that Fcγ receptor-mediated phagocytosis required PI3K-induced actin polymerization. They found that the PI3K inhibitors, LY294002 and wortmannin, prevented Fcγ receptor-mediated phagocytosis and pseudopod extension. Importantly, LY294002 and wortmannin only inhibited the phagocytosis of particles greater than 3μm suggesting that PI3K is necessary for engulfment of particles greater than 3μm but not smaller ones [51]. This size-dependent effect may explain the lack of PI3K involvement in MerTK endocytosis, as the MerTK-induced PI3K activity may only be required for internalization of particulate targets.

Much to our surprise Src-family kinase/Syk inhibition had no impact on MerTK endocytosis (Figure 9E and 9D, respectively). This was surprising as inhibition of these proteins typically blocks internalization through most phagocytic receptors independent of particle size, including in assays of antibody-mediated receptor crosslinking [19,58,80]. Oddly, Src-family kinase and Syk inhibition reduced total phosphorylation induced by MerTK crosslinking (Figure 12F and 12E, respectively) suggesting that while MerTK was activating the Src-family kinase/Syk kinase pathway, a novel Src-family kinase/Syk independent pathway was being used to mediate MerTK internalization. Given these results, I predict that future studies using a MerTK-specific bead-based assay will identify a role of PI3K for engulfment of MerTK-specific particles greater than 3μm in diameter, while Src-family kinase/Syk will not be involved in the uptake of these particulate targets.

The signalling patterns of MerTK varied from that used by Fcγ receptors in more than the requirement for Src/Syk-family kinases. Indeed, both immunofluorescence and immunoblotting revealed that MerTK had a much smaller impact on the change in protein phosphorylation than did Fcγ receptor signalling (Figures 11B, 11C, and Figure 13). Immunoblotting confirmed that MerTK activation led to phosphorylation of a smaller number of proteins than did aggregated IgG (Figure 13), and moreover, increased phosphorylation was observed only proximal to MerTK without significant changes

observed at the whole cell level (Figure 11C and 11E). This suggests that MerTK is phosphorylating only a small portion of proximal proteins, without the cell-wide changes in phosphorylation patterns observed downstream of Fcγ receptor engagement. I attempted to identify these MerTK-phosphorylated proteins using a phosphotyrosine immunoprecipitation (Figure 14), but the low level of protein phosphorylation induced by endogenous MerTK stymied this experiment. Therefore, in the future we aim to generate cells ectopically expressing MerTK at a high level, allowing for an induction of MerTK-dependent phosphorylation that is sufficient for phosphotyrosine immunoprecipitation.

4.4 Implications of MerTK signalling in health and disease

It is evident that MerTK plays an important role in efferocytosis and homeostasis as MerTK mutations are associated with the accumulation of apoptotic cells, development of lupus-like autoimmunity, and worsening of inflammatory diseases such as atherosclerosis [3,42,43,71]. We have discovered that MerTK is expressed in M0 and M2 macrophage subtypes (Figure 6), which is expected as these cell types are known to play a homeostatic role in clearing apoptotic cells and tissue remodelling after injury [81]. These findings are interesting in the context of atherosclerosis, as it is well established that M1 cells are common in the atherosclerotic plaque, suggesting that inappropriate differentiation of macrophages to an M1 phenotype within the vascular intima may be a critical step in the development of an atheroma [78,81,82].

We have also discovered that MerTK is internalized upon activation through a pathway independent of the common regulators of phagocytosis. Interestingly, a portion of the MerTK signalling is dependent on these signalling molecules, even though the internalization of MerTK is not. Although further elucidation of MerTK signalling pathway is required to better understand what is occurring, these findings suggest that anti-inflammatory or anti-autoimmune therapies targeting the Src/Syk pathway should not impair efferocytosis through MerTK. Such therapies may be of great benefit, given the central role of Src-family kinase and Syk in mediating inflammatory processes [83]. Indeed, there is strong evidence linking Src-family kinases to acute inflammatory signalling, with animal studies demonstrating that inhibitors of Src-family kinases reduce acute inflammation and tissue injury [83–85].

Our data also has implication in autoimmune disease. Previous studies have shown that knockout mice lacking MerTK or its opsonins develop autoimmune disease, suggestive that any defect in MerTK signalling may result in autoimmunity [3]. Indeed, we hope that our continued study of MerTK signalling may identify critical signalling pathways which become impaired during the induction of autoimmunity. Identification of these pathways may lead to pharmacological targets for prevention or treatment of autoimmune disease. One such pathway may be the Src/Syk pathway assessed in this thesis. Indeed, we observed that MerTK induced phosphorylation via Src-family kinase and Syk, but that MerTK internalization was independent of these kinases. If this observation holds true, this may offer to opportunity to inhibit autoimmune responses by blocking components of the Src-family kinase/Syk signalling pathway without blocking efferocytosis. This would therefore allow us to block Src-family kinase signalling, which is previously established to be associated with autoimmunity [86], without reducing the clearance of apoptotic cells and thus avoiding further complications due to poor apoptotic cell clearance.

PI3K is also linked with inflammation and autoimmunity, for instance Barber *et al.* [87] and Camps *et al.* [88] discovered inhibitors that blocked PI3Kγ complex, reduced glomerulonephritis, lupus, and rheumatoid arthritis in mouse models. However, PI3K is not as viable a target as it may be required for the uptake of particulate targets, and therefore PI3K inhibition may block some aspects of autoimmunity while at the same time augment autoantigen and alarmin release through reducing efferocytosis.

Lastly, because MerTK is internalized independently of the commonly used Src/Syk pathway, full elucidation of the MerTK signalling pathway will require an undirected approach such as the immunoprecipitation of tyrosine-phosphorylated proteins attempted in my final objective (Figure 14). Such an assay would allow for identification of the pathways lying downstream of MerTK activation, with follow-up assays such as siRNA knockdown of the identified signalling molecules used to assess the role of the proteins in MerTK-mediated efferocytosis. The significance of these future studies is that they will provide insights into MerTK's function under homeostatic conditions, and ultimately provide the knowledge necessary to understand how MerTK is dysfunctional under inflammatory (example, atherosclerotic) or autoimmune conditions. This research has the

potential to identify novel therapeutic and preventative strategies for inflammatory and autoimmune diseases through reversing defects in MerTK function or otherwise altering MerTK-dependent signalling.

References

1. Schutters, K. *et al.* Cell surface-expressed phosphatidylserine as therapeutic target to enhance phagocytosis of apoptotic cells. *Cell Death Differ.* **20,** 49–56 (2013).

2. Van Vré, E. a, Ait-Oufella, H., Tedgui, A. & Mallat, Z. Apoptotic cell death and efferocytosis in atherosclerosis. *Arterioscler. Thromb. Vasc. Biol.* **32,** 887–889 (2012).

3. Cohen, P. L. *et al.* Delayed Apoptotic Cell Clearance and Lupus-like Autoimmunity in Mice Lacking the c-mer Membrane Tyrosine Kinase. *J. Exp. Med.* **196,** 135–140 (2002).

4. Kerr, J. F. R., Wyllie, A. H., & Currie, A. R. Apoptosis: A basic biological phenomenon with wide-ranging implications in tissue kinetics. *Br. J. Cancer* **26,** 239–257 (1972).

5. Parrish, A. B., Freel, C. D. & Kornbluth, S. Cellular mechanisms controlling caspase activation and function. *Cold Spring Harb. Perspect. Biol.* **5,** 1–24 (2013).

6. Cullen, S. P. & Martin, S. J. Caspase activation pathways: some recent progress. *Cell Death Differ.* **16,** 935–8 (2009).

7. Nagata, S., Hanayama, R. & Kawane, K. Autoimmunity and the clearance of dead cells. *Cell* **140,** 619–30 (2010).

8. Nagata, S., Nagase, H., Kawane, K., Mukae, N. & Fukuyama, H. Degradation of chromosomal DNA during apoptosis. *Cell Death Differ.* **10,** 108–16 (2003).

9. Wickman, G., Julian, L. & Olson, M. F. How apoptotic cells aid in the removal of their own cold dead bodies. *Cell Death Differ.* **19,** 735–742 (2012).

10. Coleman, M. L. *et al.* Membrane blebbing during apoptosis results from caspase-mediated activation of ROCK I. *Nat. Cell Biol.* **3,** 339–45 (2001).

11. Ravichandran, K. S. Find-me and eat-me signals in apoptotic cell clearance: progress and conundrums. *J. Exp. Med.* **207,** 1807–17 (2010).

12. Peter, C. *et al.* Migration to apoptotic "find-me" signals is mediated via the phagocyte receptor G2A. *J. Biol. Chem.* **283,** 5296–305 (2008).

13. Elliott, M. R. *et al.* Nucleotides released by apoptotic cells act as a find-me signal to promote phagocytic clearance. *Nature* **461,** 282–286 (2010).

14. Hochreiter-Hufford, A. & Ravichandran, K. S. Clearing the dead: apoptotic cell sensing, recognition, engulfment, and digestion. *Cold Spring Harb. Perspect. Biol.* **5,** 1–19 (2013).

15. Erwig, L.-P. & Henson, P. M. Clearance of apoptotic cells by phagocytes. *Cell Death Differ.* **15,** 243–50 (2008).

16. Flannagan, R. S., Jaumouillé, V. & Grinstein, S. The cell biology of phagocytosis. *Annu. Rev. Pathol.* **7,** 61–98 (2012).

17. Lentz, B. R. Exposure of platelet membrane phosphatidylserine regulates blood coagulation. *Prog. Lipid Res.* **42,** 423–438 (2003).

18. Gardai, S. J. *et al.* Cell-surface calreticulin initiates clearance of viable or apoptotic cells through trans-activation of LRP on the phagocyte. *Cell* **123,** 321–34 (2005).

19. Heit, B. *et al.* Multimolecular Signaling Complexes Enable Syk-Mediated Signaling of CD36 Internalization. *Dev. Cell* **24,** 372–83 (2013).

20. Poon, I. K. H., Hulett, M. D. & Parish, C. R. Molecular mechanisms of late apoptotic/necrotic cell clearance. *Cell Death Differ.* **17,** 381–97 (2010).

21. Park, D. *et al.* BAI1 is an engulfment receptor for apoptotic cells upstream of the ELMO/Dock180/Rac module. *Nature* **450,** 430–4 (2007).

22. Kobayashi, N. *et al.* TIM-1 and TIM-4 glycoproteins bind phosphatidylserine and mediate uptake of apoptotic cells. *Immunity* **27,** 927–40 (2007).

23. Park, S.-Y. *et al.* Rapid cell corpse clearance by stabilin-2, a membrane phosphatidylserine receptor. *Cell Death Differ.* **15,** 192–201 (2008).

24. Fairn, G. D. & Grinstein, S. How nascent phagosomes mature to become phagolysosomes. *Trends Immunol.* **33,** 397–405 (2012).

25. Sather, S. *et al.* A soluble form of the Mer receptor tyrosine kinase inhibits macrophage clearance of apoptotic cells and platelet aggregation. *Blood* **109,** 1026–33 (2007).

26. Shelby, S. J., Colwill, K., Dhe-Paganon, S., Pawson, T. & Thompson, D. a. MERTK interactions with SH2-domain proteins in the retinal pigment epithelium. *PLoS One* **8,** 1–14 (2013).

27. Behrens, E. M. *et al.* The mer receptor tyrosine kinase: expression and function suggest a role in innate immunity. *Eur. J. Immunol.* **33,** 2160–7 (2003).

28. Verma, A., Warner, S. L., Vankayalapati, H., Bearss, D. J. & Sharma, S. Targeting Axl and Mer kinases in cancer. *Mol. Cancer Ther.* **10,** 1763–73 (2011).

29. Chen, C. *et al.* Mer receptor tyrosine kinase signaling participates in platelet function. *Arterioscler. Thromb. Vasc. Biol.* **24,** 1118–23 (2004).

30. Aoba, A. Promotion Product of the of Growth Uptake of PS Liposomes Apoptotic Cells by a Interaction of Gas6 with PS-To determine the binding specificity of Gas6 to liposomes , we analyzed the binding activity of Gas6 to lipids with the same lipid composition as. *Japanese Biochem. Soc.* **127,** 411–417 (2000).

31. Caberoy, N. B., Zhou, Y. & Li, W. Tubby and tubby-like protein 1 are new MerTK ligands for phagocytosis. *EMBO J.* **29,** 3898–910 (2010).

32. Ling, L., Templeton, D. & Kung, H.-J. Identification of the Major Autophosphorylation Sites of Nyk/Mer, an NCAM-related Receptor Tyrosine Kinase. *J. Biol. Chem.* **271,** 18355–18362 (1996).

33. Tibrewal, N. *et al.* Autophosphorylation docking site Tyr-867 in Mer receptor tyrosine kinase allows for dissociation of multiple signaling pathways for phagocytosis of apoptotic cells and down-modulation of lipopolysaccharide-inducible NF-kappaB transcriptional activation. *J. Biol. Chem.* **283,** 3618–27 (2008).

34. Kevany, B. M. *et al.* Phagocytosis of Retinal Rod and Cone Photoreceptors progressive retinal degeneration Phagocytosis of Retinal Rod and Cone Photoreceptors. *Physiology* **25,** 8–15 (2012).

35. D'Cruz, P. M. *et al.* Mutation of the receptor tyrosine kinase gene Mertk in the retinal dystrophic RCS rat. *Hum. Mol. Genet.* **9,** 645–51 (2000).

36. Duncan, J. L. An RCS-Like Retinal Dystrophy Phenotype in Mer Knockout Mice. *Invest. Ophthalmol. Vis. Sci.* **44,** 826–838 (2003).

37. Gal, A. *et al.* Mutations in MERTK, the human orthologue of the RCS rat retinal dystrophy gene, cause retinitis pigmentosa. *Nat. Genet.* **26,** 270 – 271 (2000).

38. Gregory, C. D. & Pound, J. D. Cell death in the neighbourhood: direct microenvironmental effects of apoptosis in normal and neoplastic tissues. *J. Pathol.* **223,** 177–94 (2011).

39. Baumann, I. *et al.* Impaired Uptake of Apoptotic Cells Into Tingible Body Macrophages in Germinal Centers of Patients With Systemic Lupus Erythematosus. *Arthritis Rheum.* **46,** 191–201 (2002).

40. Recarte-Pelz, P. *et al.* Vitamin K-dependent proteins GAS6 and Protein S and TAM receptors in patients of systemic lupus erythematosus: correlation with common genetic variants and disease activity. *Arthritis Res. Ther.* **15,** 1–9 (2013).

41. Thorp, E. & Tabas, I. Mechanisms and consequences of efferocytosis in advanced atherosclerosis. *J. Leukoc. Biol.* **86,** 1089–1095 (2009).

42. Ait-Oufella, H. *et al.* Defective mer receptor tyrosine kinase signaling in bone marrow cells promotes apoptotic cell accumulation and accelerates atherosclerosis. *Arterioscler. Thromb. Vasc. Biol.* **28,** 1429–31 (2008).

43. Thorp, E., Cui, D., Schrijvers, D. M., Kuriakose, G. & Tabas, I. Mertk receptor mutation reduces efferocytosis efficiency and promotes apoptotic cell accumulation and plaque necrosis in atherosclerotic lesions of apoe-/- mice. *Arterioscler. Thromb. Vasc. Biol.* **28,** 1421–8 (2008).

44. Thorp, E., Subramanian, M. & Tabas, I. The role of macrophages and dendritic cells in the clearance of apoptotic cells in advanced atherosclerosis. *Eur. J. Immunol.* **41,** 2515–8 (2011).

45. Hurtado, B. *et al.* Association study between polymorphims in GAS6-TAM genes and carotid atherosclerosis. *Thromb. Haemost.* **104,** 592–598 (2010).

46. Hurtado, B. & Munoz, X. Expression of the vitamin K-dependent proteins GAS6 and protein S and the TAM receptor tyrosine kinases in human atherosclerotic carotid plaques. *Thromb. Haemost.* **105,** 873–882 (2011).

47. Guilliams, M., Bruhns, P., Saeys, Y., Hammad, H. & Lambrecht, B. N. The function of Fcγ receptors in dendritic cells and macrophages. *Nat. Rev. Immunol.* **14,** 94–108 (2014).

48. García-García, E. & Rosales, C. Signal transduction during Fc receptor-mediated phagocytosis. *J. Leukoc. Biol.* **72,** 1092–108 (2002).

49. Hunter, S. *et al.* Inhibition of Fcgamma receptor-mediated phagocytosis by a nonphagocytic Fcgamma receptor. *Blood* **91,** 1762–8 (1998).

50. Crowley, M. T. *et al.* A critical role for Syk in signal transduction and phagocytosis mediated by Fcgamma receptors on macrophages. *J. Exp. Med.* **186,** 1027–39 (1997).

51. Cox, D., Tseng, C.-C., Bjekic, G. & Greenberg, S. A Requirement for Phosphatidylinositol 3-Kinase in Pseudopod Extension. *J. Biol. Chem.* **274,** 1240–1247 (1999).

52. Fuller, G. L. J. *et al.* The C-type lectin receptors CLEC-2 and Dectin-1, but not DC-SIGN, signal via a novel YXXL-dependent signaling cascade. *J. Biol. Chem.* **282,** 12397–12409 (2007).

53. Mócsai, A., Ruland, J. & Tybulewicz, V. L. J. The SYK tyrosine kinase: a crucial player in diverse biological functions. *Nat Rev Immunol* **10,** 387–402 (2010).

54. Takada, Y., Ye, X. & Simon, S. The integrins. *Genome Biol.* **8,** 215–219 (2007).

55. Ross, R. S. & Borg, T. K. Integrins and the Myocardium. *Circ. Res.* **88,** 1112–1119 (2001).

56. Wiedemann, A. *et al.* Two distinct cytoplasmic regions of the beta2 integrin chain regulate RhoA function during phagocytosis. *J. Cell Biol.* **172,** 1069–79 (2006).

57. Schwartz, M. A. & Assoian, R. K. Integrins and cell proliferation: regulation of cyclin-dependent kinases via cytoplasmic signaling pathways. *J. Cell Sci.* **114,** 2553–60 (2001).

58. Wu, Y., Singh, S., Georgescu, M.-M. & Birge, R. B. A role for Mer tyrosine kinase in alphavbeta5 integrin-mediated phagocytosis of apoptotic cells. *J. Cell Sci.* **118,** 539–53 (2005).

59. Finnemann, S. C. & Nandrot, E. F. MerTK activation during RPE phagocytosis in vivo requires αVβ5 integrin. *Adv. Exp. Med. Biol.* **572,** 499–503 (2006).

60. Dupuy, A. G. & Caron, E. Integrin-dependent phagocytosis: spreading from microadhesion to new concepts. *J. Cell Sci.* **121,** 1773–83 (2008).

61. Lowell, A., Chu, C., Killebrew, J. ., Ni, M. & Hamerman, J. . The expanding roles of ITAM adapters FcRγ and DAP12 in myeloid cells. *Immunol. Rev.* **232,** 42–58 (2009).

62. Finnemann, S. C. & Rodriguez-boulan, E. Macrophage and Retinal Pigment Epithelium Phagocytosis: Apoptotic Cells and Photoreceptors Compete for αvβ3 and αvβ5 Integrins, and Protein Kinase C Regulates αvβ5 Binding and Cytoskeletal Linkage. *J. Exp. Med.* **190,** 861–874 (1999).

63. Edelstein, A., Amodaj, N., Hoover, K., Vale, R. & Stuurman, N. Computer control of microscopes using μManager. *Curr. Protoc. Mol. Biol.* **14,** 1–17 (2010).

64. Bolte, S. & Cordelières, F. P. A guided tour into subcellular colocalization analysis in light microscopy. *J. Microsc.* **224,** 213–232 (2010).

65. Flannagan, R. S., Harrison, R. E., Yip, C. M., Jaqaman, K. & Grinstein, S. Dynamic macrophage "probing" is required for the efficient capture of phagocytic targets. *J. Cell Biol.* **191,** 1205–1218 (2010).

66. Botelho, R. J. *et al.* Localized biphasic changes in phosphatidylinositol-4,5-bisphosphate at sites of phagocytosis. *J. Cell Biol.* **151,** 1353–68 (2000).

67. Fairn, G. D. *et al.* An electrostatic switch displaces phosphatidylinositol phosphate kinases from the membrane during phagocytosis. *J. Cell Biol.* **187,** 701–14 (2009).

68. Todt, J. C., Hu, B. & Curtis, J. L. The scavenger receptor SR-A I/II (CD204) signals via the receptor tyrosine kinase Mertk during apoptotic cell uptake by murine macrophages. *J. Leukoc. Biol.* **84,** 510–8 (2008).

69. Mero, P. *et al.* Phosphorylation-independent ubiquitylation and endocytosis of Fc gammaRIIA. *J. Biol. Chem.* **281,** 33242–9 (2006).

70. Feng, W., Yasumura, D., Matthes, M. T., LaVail, M. M. & Vollrath, D. Mertk triggers uptake of photoreceptor outer segments during phagocytosis by cultured retinal pigment epithelial cells. *J. Biol. Chem.* **277,** 17016–22 (2002).

71. Wan, E. *et al.* Enhanced efferocytosis of apoptotic cardiomyocytes through myeloid-epithelial-reproductive tyrosine kinase links acute inflammation resolution to cardiac repair after infarction. *Circ. Res.* **113,** 1004–12 (2013).

72. Jensen, K. D. C. *et al.* Toxoplasma polymorphic effectors determine macrophage polarization and intestinal inflammation. *Cell Host Microbe* **9,** 472–83 (2011).

73. Gairin, J. Expression in yeast of a cDNA clone encoding a transmembrane glycoprotein gp41 fragment (a.a. 591–642) bearing the major immunodominant domain of human immunodeficiency virus. *FEMS Microbiol. Lett.* **76,** 109–119 (1991).

74. Balce, D. R. *et al.* Alternative activation of macrophages by IL-4 enhances the proteolytic capacity of their phagosomes through synergistic mechanisms. *Blood* **118,** 4199–208 (2011).

75. Cassol, E., Cassetta, L., Rizzi, C., Alfano, M. & Poli, G. M1 and M2a polarization of human monocyte-derived macrophages inhibits HIV-1 replication by distinct mechanisms. *J. Immunol.* **182,** 6237–46 (2009).

76. Recalcati, S. *et al.* Differential regulation of iron homeostasis during human macrophage polarized activation. *Eur. J. Immunol.* **40,** 824–35 (2010).

77. Banerjee, S. *et al.* MicroRNA let-7c Regulates Macrophage Polarization. *J. Immunol.* **190,** 6542–6549 (2013).

78. Zizzo, G., Hilliard, B. a, Monestier, M. & Cohen, P. L. Efficient Clearance of Early Apoptotic Cells by Human Macrophages Requires M2c Polarization and MerTK Induction. *J. Immunol.* **189,** 3508–20 (2012).

79. Nandrot, E. F. *et al.* Essential role for MFG-E8 as ligand for alphavbeta5 integrin in diurnal retinal phagocytosis. *Proc. Natl. Acad. Sci. U. S. A.* **104,** 12005–10 (2007).

80. Majeed, M., Caveggion, E., Lowell, C. A. & Berton, G. Role of Src kinases and Syk in Fcγ receptor-mediated phagocytosis and phagosome-lysosome fusion. *J. Leukoc. Biol.* **70,** 801–811 (2001).

81. Taylor, P. R. *et al.* Macrophage receptors and immune recognition. *Annu. Rev. Immunol.* **23,** 901–44 (2005).

82. Scull, C. M., Hays, W. D. & Fischer, T. H. Macrophage pro-inflammatory cytokine secretion is enhanced following interaction with autologous platelets. *J. Inflamm. (Lond).* **7,** 53 (2010).

83. Korade-Mirnics, Z. & Corey, S. J. Src kinase-mediated signaling in leukocytes. *J. Leukoc. Biol.* **68,** 603–13 (2000).

84. Okutani, D., Lodyga, M., Han, B. & Liu, M. Src protein tyrosine kinase family and acute inflammatory responses. *Am. J. Physiol.* **291,** 129–141 (2006).

85. Ingley, E. Src family kinases: regulation of their activities, levels and identification of new pathways. *Biochim. Biophys. Acta* **1784,** 56–65 (2008).

86. Berton, G., Mócsai, A. & Lowell, C. a. Src and Syk kinases: key regulators of phagocytic cell activation. *Trends Immunol.* **26,** 208–14 (2005).

87. Barber, D. F. *et al.* PI3Kgamma inhibition blocks glomerulonephritis and extends lifespan in a mouse model of systemic lupus. *Nat. Med.* **11,** 933–5 (2005).

88. Camps, M. *et al.* Blockade of PI3Kgamma suppresses joint inflammation and damage in mouse models of rheumatoid arthritis. *Nat. Med.* **11,** 936–43 (2005).

Appendix

Figure A1: Plasmid maps of source and attempted MerTk mammalian expression vectors. A-B) – source vectors for murine **(A)** pIRES2-EGFP MerTK from Addgene, and human **(B)** pDONR233-MerTK from Addgene. **C-E)** attempted MerTK expression vectors: **C)** Wild-type murine MerTK, **D)** GFP murine MerTK and **E)** wild-type human MerTK. Plasmid maps A-B are from Addgene, all others were created with SnapGene software.

A)

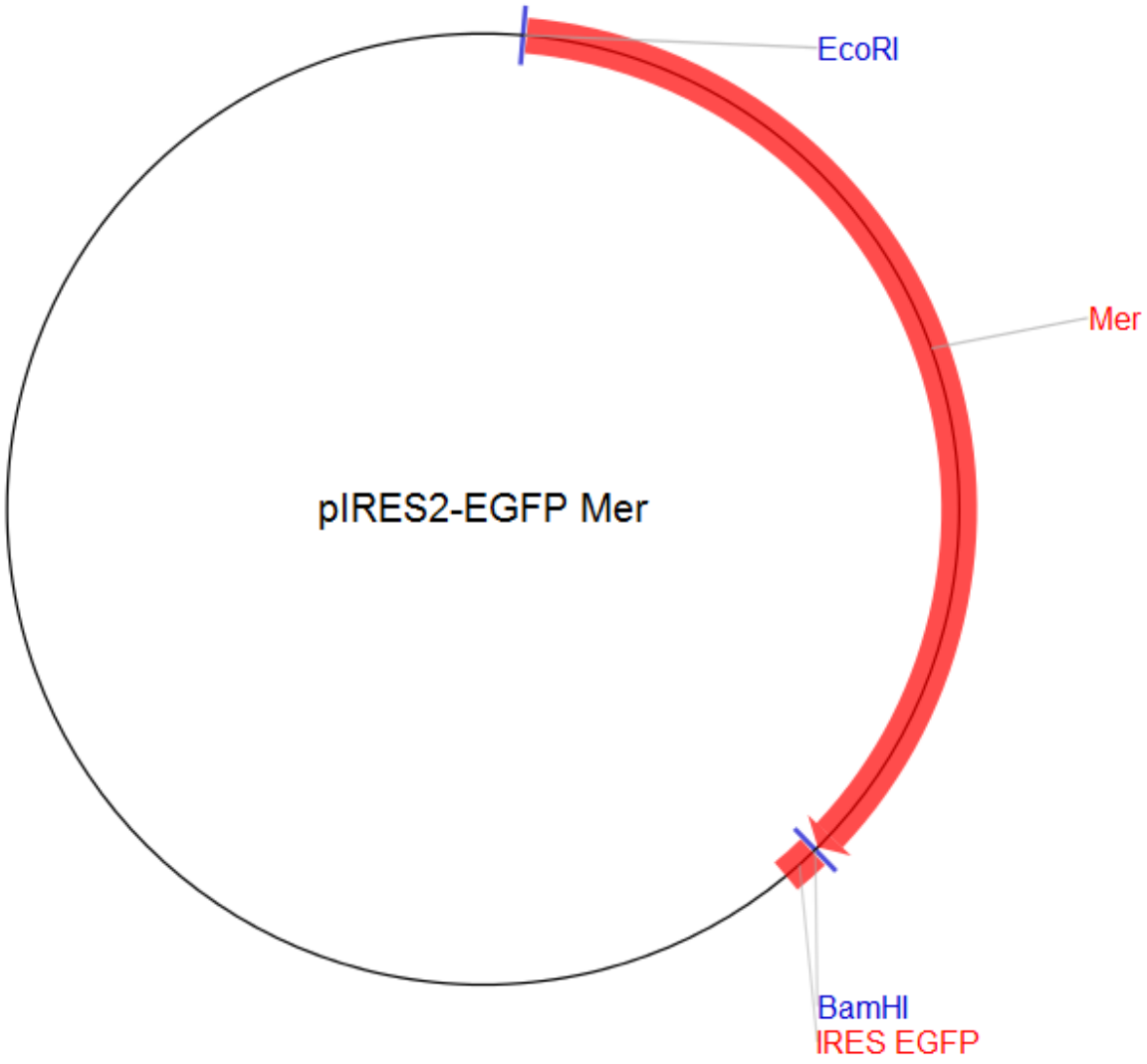

B)

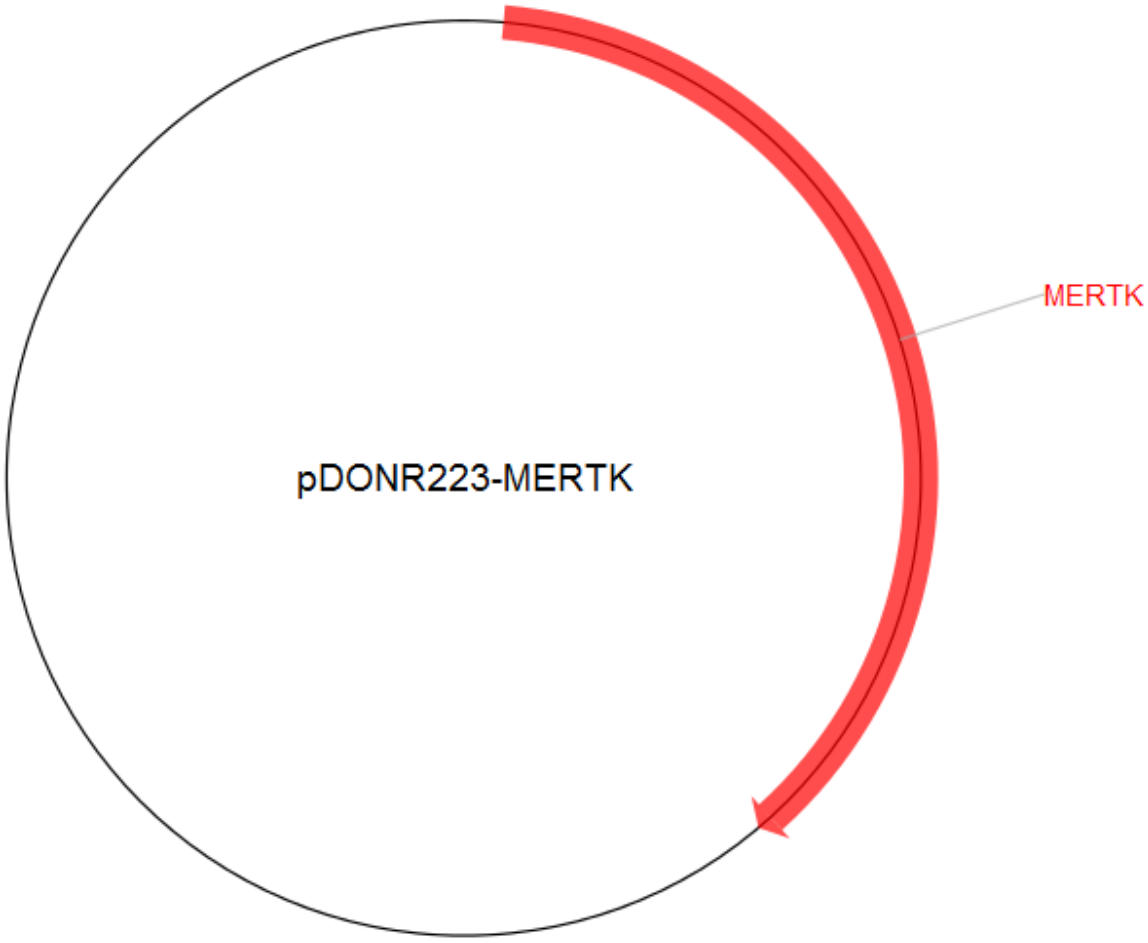

C)

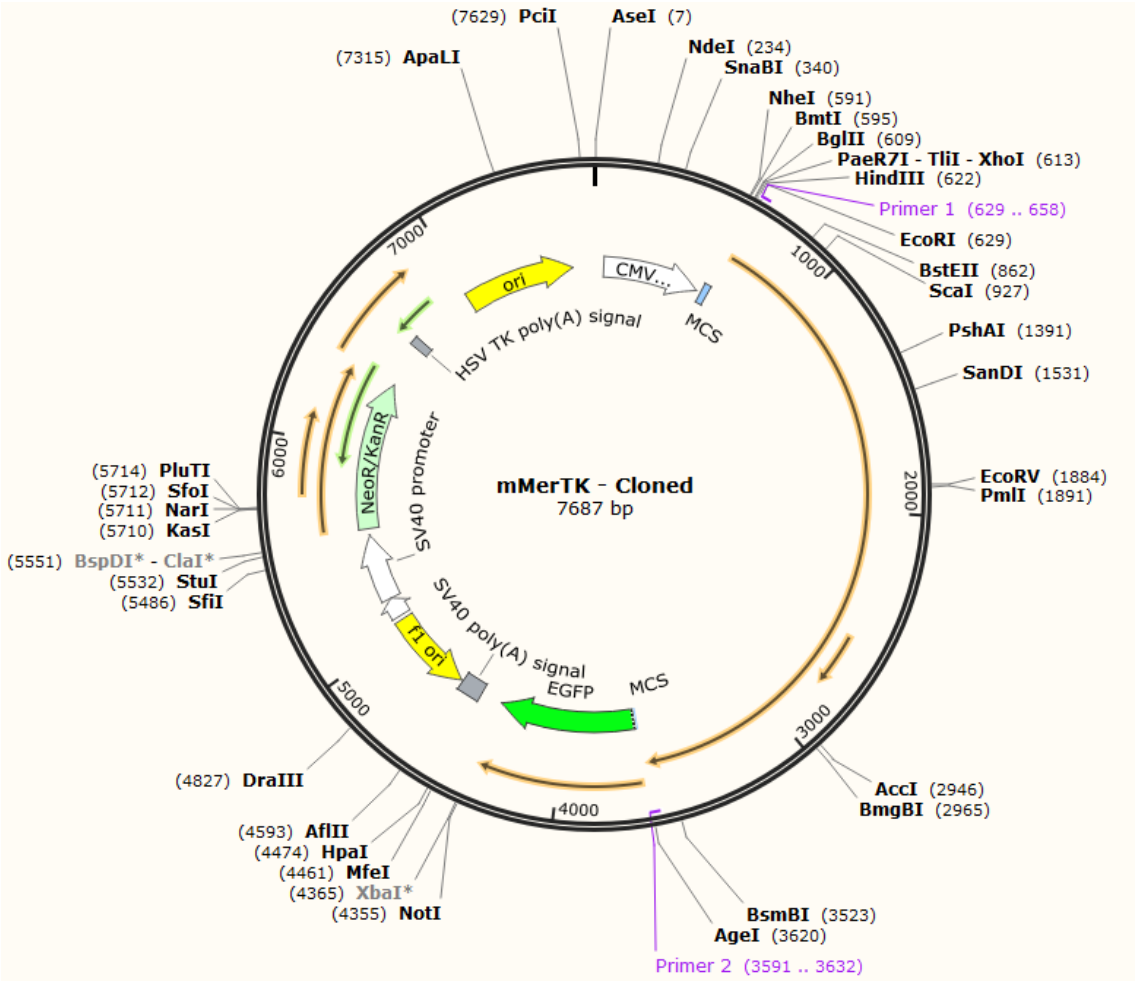
(7629) PciI
AseI (7)
(7315) ApaLI
NdeI (234)
SnaBI (340)
NheI (591)
BmtI (595)
BglII (609)
PaeR7I - TliI - XhoI (613)
HindIII (622)
Primer 1 (629 .. 658)
EcoRI (629)
BstEII (862)
ScaI (927)
PshAI (1391)
SanDI (1531)
EcoRV (1884)
PmlI (1891)
AccI (2946)
BmgBI (2965)
BsmBI (3523)
AgeI (3620)
Primer 2 (3591 .. 3632)
(4827) DraIII
(4593) AflII
(4474) HpaI
(4461) MfeI
(4365) XbaI*
(4355) NotI
(5714) PluTI
(5712) SfoI
(5711) NarI
(5710) KasI
(5551) BspDI* - ClaI*
(5532) StuI
(5486) SfiI
7000
1000
2000
3000
4000
5000
6000
ori
CMV...
MCS
HSV TK poly(A) signal
NeoR/KanR
SV40 promoter
mMerTK - Cloned
7687 bp
f1 ori
SV40 poly(A) signal
EGFP
MCS

D)

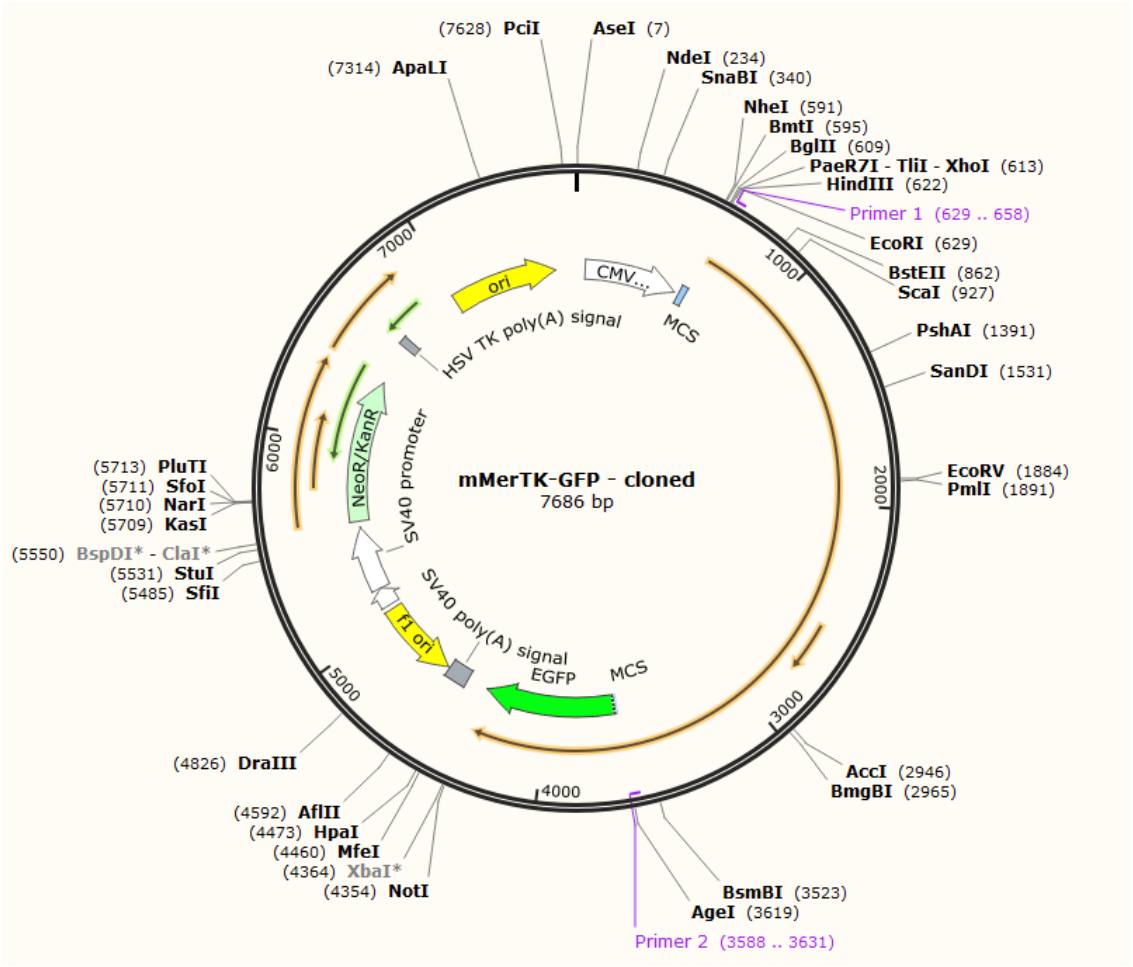
(7628) PciI
AseI (7)
(7314) ApaLI
NdeI (234)
SnaBI (340)
NheI (591)
BmtI (595)
BglII (609)
PaeR7I - TliI - XhoI (613)
HindIII (622)
Primer 1 (629 .. 658)
EcoRI (629)
BstEII (862)
ScaI (927)
PshAI (1391)
SanDI (1531)
EcoRV (1884)
PmlI (1891)
AccI (2946)
BmgBI (2965)
BsmBI (3523)
AgeI (3619)
Primer 2 (3588 .. 3631)
(4826) DraIII
(4592) AflII
(4473) HpaI
(4460) MfeI
(4364) XbaI*
(4354) NotI
(5713) PluTI
(5711) SfoI
(5710) NarI
(5709) KasI
(5550) BspDI* - ClaI*
(5531) StuI
(5485) SfiI
ori
CMV...
MCS
HSV TK poly(A) signal
NeoR/KanR
SV40 promoter
mMerTK-GFP - cloned
7686 bp
SV40 poly(A) signal
f1 ori
EGFP
MCS
1000
2000
3000
4000
5000
6000
7000

E)

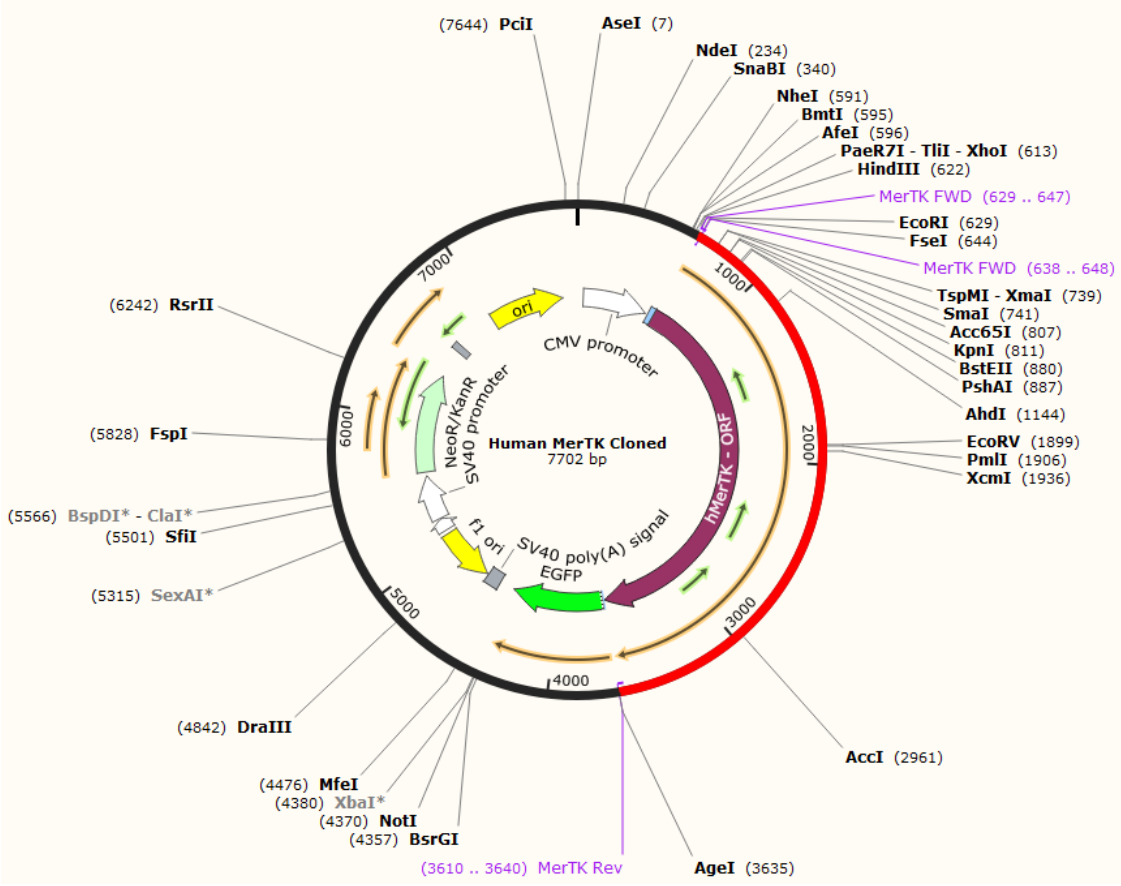
(7644) PciI
AseI (7)
NdeI (234)
SnaBI (340)
NheI (591)
BmtI (595)
AfeI (596)
PaeR7I - TliI - XhoI (613)
HindIII (622)
MerTK FWD (629 .. 647)
EcoRI (629)
FseI (644)
MerTK FWD (638 .. 648)
TspMI - XmaI (739)
SmaI (741)
Acc65I (807)
KpnI (811)
BstEII (880)
PshAI (887)
AhdI (1144)
EcoRV (1899)
PmlI (1906)
XcmI (1936)
AccI (2961)
AgeI (3635)
(3610 .. 3640) MerTK Rev
(4357) BsrGI
(4370) NotI
(4380) XbaI*
(4476) MfeI
(4842) DraIII
(5315) SexAI*
(5501) SfiI
(5566) BspDI* - ClaI*
(5828) FspI
(6242) RsrII
1000
2000
3000
4000
5000
6000
7000
ori
CMV promoter
hMerTK - ORF
SV40 poly(A) signal
EGFP
f1 ori
NeoR/KanR
SV40 promoter
Human MerTK Cloned
7702 bp

Curriculum Vitae

Name:	Ekenedelichukwu Azu
Post-secondary Education and Degrees:	University of Ontario Institute of Technology (UOIT); Oshawa, Ontario, Canada 2008-2012, B.HSc, honours. (Medical Laboratory Science) University of Western Ontario; London, Ontario, Canada 2012-2014, M.Sc. (Microbiology and Immunology)
Academic Achievements:	President's list on Medical Laboratory Science Program of UOIT (2010-2012) Dean's list on Medical Laboratory Science Program of UOIT (2009)
Presentation and Talks:	London Health Research Day, London, Ontario, Canada (2013, 2014). Poster presentation: Elucidating the signalling pathway of Mer tyrosine kinase in efferocytosis. Infection and Immunity Research Forum, London, Ontario, Canada (2012, 2013). Poster presentation: Elucidating the signalling pathway of Mer tyrosine kinase in efferocytosis.